THESIS FOR THE DEGREE OF DOCTOR OF PHILOSOPHY

Strengthening reinforced concrete structures with FRP composites

JINCHENG YANG

Department of Architecture and Civil Engineering

CHALMERS UNIVERSITY OF TECHNOLOGY

Gothenburg, Sweden 2021

Strengthening reinforced concrete structures with FRP composites

JINCHENG YANG

ISBN 978-91-7905-452-6

Doktorsavhandlingar vid Chalmers tekniska högskola
Ny serie nr 4919
ISSN 0346-718X

Department of Architecture and Civil Engineering
Chalmers University of Technology
SE-412 96 Gothenburg
Sweden
Telephone + 46 (0)31-772 1000

Cover:
[An existing RC bridge strengthened with a hybrid FRP strengthening system proposed in the research project SUREBRIDGE as part of the work of this thesis]

Chalmers Reproservice
Gothenburg, Sweden 2021

To my parents

Strengthening reinforced concrete structures with FRP composites
JINCHENG YANG
Department of Architecture and Civil Engineering
Division of Structural Engineering
Chalmers University of Technology

ABSTRACT

Civil infrastructures made of reinforced concrete (RC) play an important role in the economic activities and services of society. However, signs of deterioration and functional deficiency are commonly found in existing RC structures. Thus, there is a great demand for upgrading the capacity and performance of existing concrete structures. Fibre reinforced polymer (FRP) composites have been widely used as externally bonded reinforcement (EBR) for strengthening RC structures since the 1990s. The work of this thesis aimed to investigate robust and efficient FRP-strengthening systems for structural strengthening of existing RC structures with a focus on RC bridge superstructures. Three different strengthening techniques were investigated.

A recently developed technique, namely the stepwise prestressing method, was studied in the current work to eliminate the need for mechanical anchors when using prestressed carbon-FRP (CFRP) plate as EBR for strengthening RC beams. Experiments showed that this method could realise the self-anchorage of prestressed CFRP plates on the surface of concrete beams given prestressing levels of 25-30% (of the CFRP tensile capacity). Despite no installation of mechanical anchors, the self-anchored prestressed plates were demonstrated to be efficient in reducing crack widths and improving the flexural capacity of the strengthened RC beams. At the debonding of the CFRP plates, the utilization ratios were in the range of 81-86% (of the CFRP tensile capacity) indicating significantly improved utilisation of the plates compared with equivalent non-prestressed plates.

A practical modelling strategy was also developed to enable nonlinear FEA of the CFRP-strengthened RC beam. Using the FEA, parametric studies on the self-anchored plates indicated an optimal prestressing level of 40% (specifically for the investigated specimen), above which both load-carrying and deflection capacities of the strengthened beam would decrease due to CFRP debonding before yielding of steel reinforcement.

A hybrid FRP system for strengthening RC beams with a T-shaped cross-section, representing the deck and girder system of RC bridge superstructures, was also investigated. The hybrid system included self-anchored prestressed CFRP plates applied to the soffit of the T-beams and prefabricated glass-FRP (GFRP) panels installed on the top of the T-beam flanges. In the strengthened RC T-beams subjected to bending, the CFRP plate acted as tensile reinforcement and the GFRP panel took most of the compressive force. Flexural tests showed that the applied hybrid FRP strengthening system was robust and efficient in improving the flexural stiffness and capacity. The tests also highlighted substantial residual capacity after the CFRP debonding, as the compressive zone shifted to the GFRP panel and concrete crushing at the top of the T-beam was prevented.

The current work also investigated effective FRP strengthening systems for deteriorated concrete beams with highly corroded steel reinforcement. The system included externally bonded FRP reinforcement on the beam soffit and CFRP U-jackets along the span. Flexural

tests showed that the system was efficient in upgrading the flexural capacity of deteriorated concrete beams, despite local corrosion levels of steel reinforcement up to 57% and unrepaired concrete cover with up to 2 mm wide corrosion-induced cracks. The U-jackets effectively suppressed spalling of the concrete cover and thus enabled improved utilisation of the bonded FRP reinforcement on the beam soffits, with a utilisation ratio of CFRP plates up to 64% and even rupture of GFRP laminates.

In summary, the FRP-strengthening systems investigated in the current work were demonstrated to be robust and efficient in strengthening RC members subjected to bending.

Keywords:
Fibre reinforced polymer, CFRP, GFRP, externally bonded reinforcement, prestressing level, debonding, self-anchorage, interfacial stress, concrete structures, corrosion, finite element analysis.

TABLE OF CONTENTS

PREFACE

The work presented in this doctoral thesis was carried out between April 2016 and March 2021 in the Division of Structural Engineering at Chalmers University of Technology. The current work encompassed the content of two research projects, respectively, financed by Infravation [31109806.0009] (2015-2018) and Swedish Transport Administration [BBT-2018-011] (2019-2022).

First, I want to express my sincere thanks to my main supervisor Assoc. Prof. Reza Haghani. Reza has been my supervisor since I was doing my master thesis at Chalmers. His supervision, patience, and encouragement have supported me to gain knowledge and develop my potential during my study. I have been inspired by his vast knowledge as my supervisor and kindness as a friend. I also want to thank my examiner Assoc. Prof. Mohammad Al-Emrani for his guidance and support during my PhD study. As a generous and charming man with a great sense of humour, he has brought us an enjoyable atmosphere in our research group.

I would like to express my honest gratitude to my co-supervisor Prof. Karin Lundgren. I am blessed to have the chance to work with her during the second half of my PhD study. I have been deeply impressed by her efficient work and sharp minds. Her constructive supervision and valuable advice are essential to the accomplishment of my current work. I would also like to thank my co-supervisor Adj. Prof. Morgan Johansson. He always keeps his door open to me and is willing to share his vast knowledge of reinforced concrete and modelling. I would also like to thank Assoc. Prof. Thomas Blanksvärd. Besides the assistance as the core member of the current research project, he has been generous to share his solid expertise in FRP-strengthening of concrete structures and willing to provide me much more help in my PhD study.

I would like to thank my former and present colleagues in our division for creating a pleasant and helpful working environment. Special thanks go to Alexandre Mathern for all our enjoyable discussion and joint work. I also want to thank Dr E Chen and Dr Carlos Gil Berrocal for their precious help in my research. I appreciate the great help from research engineers Sebastian Almfeldt, Anders Karlsson, and Tommie Månsson in all my experimental work.

I would also like to express my appreciation to Prof. Jian-Fei Chen and Dr Esmaeel Esmaeeli, who hosted and helped me during my research stay at Queen's University Belfast in May and June 2019.

Finally, I want to deliver my deep gratitude to my families. Thank my parents for all the care and support. They have taught me selflessness and kindness. Thank my wife Jiawen for her love and help during my entire PhD study. They have coloured the journal of my life.

Jincheng Yang

2021-02-25

LIST OF PUBLICATIONS

This thesis is based on the work contained in the following appended papers, referred to by Roman numerals in the text:

I. Yang J, Haghani R, Al-Emrani M. Innovative prestressing method for externally bonded CFRP laminates without mechanical anchorage. *Engineering Structures* 2019;197. doi:10.1016/j.engstruct.2019.109416.

II. Mathern A, Yang J. A practical finite element modeling strategy to capture cracking and crushing behavior of reinforced concrete structures. *Materials* 2021; 14(3):506. doi: 10.3390/ma14030506

III. Yang J, Johansson M, Al-Emrani M, Haghani R. Innovative flexural strengthening of RC beams using self-anchored prestressed CFRP plates: experimental and numerical investigations. *Submitted for publication*

IV. Yang J, Haghani R, Al-Emrani M. Flexural FRP strengthening of concrete bridges using an innovative concept. *Proceedings of the 9th International Conference on Bridge Maintenance, Safety, and Management*, 9-13 July, Melbourne, Australia: CRC Press; 2018. doi:10.1201/9781315189390.

V. Yang J, Haghani R, Blanksvärd T, Lundgren K. Experimental study of FRP-strengthened concrete beams with corroded reinforcement. *Submitted for publication*

AUTHOR'S CONTRIBUTION TO JOINTLY PUBLISHED PAPERS

The appended papers were prepared in collaboration with co-authors. The contribution by the author of this doctoral thesis to the appended papers is described below.

In **Paper I**, the author participated in the planning and execution of the experiments, carried out the FE analyses, evaluated the experimental and FE results, and took the lead in writing the paper. The co-authors of this paper contributed to the design, planning, and execution of the experiments, evaluation of the experimental and FE results, and assisted in reviewing and editing the paper.

In **Paper II**, the author provided the resources of experimental results. The author and the co-author equally contributed to planning the paper, making the literature study, performing FE analyses, evaluating the results of the FE analyses, and writing the paper associated with draft preparation, review, and editing.

In **Paper III**, the author made the literature study, participated in the planning and execution of the experiments, carried out the FE analyses, evaluated the experimental and FE results, prepared the discussion of the results, and took the lead in writing the paper. Haghani and Al-Emrani contributed to the design, planning, and execution of the experiments. Johansson supervised the FE analyses. All co-authors contributed to evaluating the results and assisted in reviewing and editing the paper.

In **Paper IV**, the author participated in the design and planning of the experiments, executed the experiments together with Haghani, carried out the analysis and evaluation of the experimental results, and took the lead in writing the paper. Haghani led the design and planning of the experiments. The co-authors of this paper contributed to evaluating the results and assisted in reviewing and editing the paper.

In **Paper V**, the author made the literature study, led the design and planning of the experiments, executed the experiments, carried out the analysis and evaluation of the experimental results, prepared the discussion of the results, and took the lead in writing the paper. The co-authors of this paper contributed to the design and planning of the experiments, the evaluation and discussion of the experimental results, and assisted in planning, reviewing, and editing the paper.

OTHER PUBLICATIONS RELATED TO THIS THESIS

In addition to the appended papers, the author of this thesis has also contributed to the following publications.

Licentiate Thesis

Yang J. Flexural Strengthening of Reinforced Concrete Beams Using Externally Bonded CFRP: An Innovative Method for the Application of Prestressed CFRP Laminates. Chalmers University of Technology, 2019.

Conference Papers

- C-I. Yang J, Haghani R, Al-Emrani M. Flexural strengthening of reinforced concrete beams using externally bonded FRP laminates prestressed with a new method. Proceedings of the 4th International Conference on Smart Monitoring, Assessment, and Rehabilitation of Civil Structures, 13-15 September, Zurich, Switzerland: 2017.
- C-II. Yang J, Haghani R, Valvo PS. A New Concept for Sustainable Refurbishment of Existing Bridges Using FRP Materials. Proceedings of the 4th International Conference on Smart Monitoring, Assessment, and Rehabilitation of Civil Structures, 13-15 September, Zurich, Switzerland: 2017.
- C-III. Atashipour R, Yang J, Haghani R. Mathematical analysis of an innovative method for strengthening concrete beams using pre-stressed FRP laminates. Proceedings of the 9th International Conference on Bridge Maintenance, Safety, and Management, 9-13 July, Melbourne, Australia: CRC Press; 2018. doi:10.1201/9781315189390.

Technical reports

- R-I. Haghani R, Yang J, Pasquale A, Ricci F, Valvo PS. SUREBRIDGE Deliverable: D2.1 Refurbishment of existing concrete and steel-concrete bridge structures. 2017. doi:10.13140/RG.2.2.29937.51046.
- R-II. Yang J, Haghani R. SUREBRIDGE Deliverable: D3.2 Preparation of Test Specimens and Experimental Program. 2017. doi:10.13140/RG.2.2.28560.97289.
- R-III. Grefhorst R, Ricci F, Valvo PS, Yang J, Haghani R, Gheorghe T, et al. SUREBRIDGE Deliverable: D3.3 Validation of the SUREBridge solution. 2017. doi:10.13140/RG.2.2.31916.41605.
- R-IV. Ricci F, Valvo PS, Bifano F, Davini E, Fisicaro P, Haghani R, Yang J, et al. SUREBRIDGE Deliverable: D4.4 Analysis of the prototype. 2018. doi:10.13140/RG.2.2.27735.50089.

1 Introduction

1.1 Background

Concrete is widely used to construct civil infrastructures encompassing bridges, dams, pavements, or buildings that are crucial to the services and economic activities of modern society. Considering that most concrete infrastructures were built in the past 50 years, more and more of these structures are approaching the end of their designed service life [1]. To meet the demands of the developing society, these concrete infrastructures require substantial maintenance or strengthening to be able to reach their designed lifetime or fulfil the intended services.

Bridges, as the critical part of road and railway networks, are good examples. In Europe, approximately 86% of bridges are made of reinforced or prestressed concrete [2]. A survey (during 2003-2005) of railway bridges in 17 European countries revealed that 80% of the bridges made of concrete were built in the past 50 years [3]. In Sweden, the age distribution of concrete bridges owned by Swedish Transport Administration showed that 40% were 20-50 years old and 34% were older than 50 years [4]. The ageing concrete bridges commonly exhibit signs of deterioration and functional deficiency even before reaching the end of their designed service life. Considering the increase in vehicle loads and traffic volume of current and future society, the ageing concrete bridges might become critical and thus fail to satisfy the demands of public traffic and safety. In Sweden, 72% of the demolished bridges during 1990-2005 were torn down due to lack of load-bearing capacity [5]. Therefore, there is a great demand for effective techniques to strengthen and modernise the functionally deficient concrete bridges.

According to feedbacks from transport agencies [4], the requirements of bridge strengthening techniques addressed not only robustness but also efficiency. A robust strengthening solution has the potential to greatly upgrade the performance of a structure above its original level. The efficiency herein means obtaining the upgraded performance at low costs in the perspectives of construction and maintenance activities, traffic disturbance, and environmental impacts. For instance, traffic closure would increase user costs due to detour or traffic congestion. The noise, vibration, and dust from the construction site cause environmental impact and thus increase social costs. With the growing public awareness of the user and social costs, traffic agencies have set a high priority for the research of non-disruptive refurbishment techniques for the repair and strengthening activities [4]. Given the fact that 70% of deterioration problems found in concrete bridges are associated with concrete decks [4], the strengthening of concrete decks and girders, acting as the main structural elements of bridge superstructures, forms a predominant part of the refurbishment of concrete bridges.

A well-established technique for strengthening concrete structures is to use fibre reinforced polymer (FRP) composites as externally bonded reinforcement [6–8]. FRP composite materials are generally comprised of high strength fibres embedded in a polymer matrix. The fibres are the main reinforcing elements, and the polymer matrix acts as a binder that protects the fibres and transfers loads between them. FRP composites are characterized by properties such as lightweight, superior strength, and high corrosion resistance. These properties closely meet the above-mentioned requirements of strengthening techniques: a) the lightweight facilitates application and thus reduce construction time, b) the high strength and stiffness mean sufficient reinforcing effects, c) the high corrosion resistance avoids the common corrosion problems of steel reinforcement and reduces the costs of inspection and maintenance during service life. In 1991, carbon-FRP (CFRP) laminates were first applied in a field project as externally bonded reinforcement for flexural strengthening of a concrete bridge in Lucerne, Switzerland [9]. Although there has been a considerable amount of studies on the externally bonded FRP reinforcement [10–20], research is still needed to bridge the gap between existing FRP-solutions and the demands for the robust and efficient strengthening of existing concrete bridges.

Pioneering studies [21,22] have shown that prestressing FRP laminates before bonding to the soffit of a concrete beam can further improve its flexural performance in terms of deflection, crack width, and ultimate capacity. To assure the function of prestressed FRP laminates, it is essential to install mechanical anchorage systems at their ends [23,24]. However, the installation of anchorage systems, e.g. the commonly used set of metallic anchor plates and bolts, is cumbersome and labour-intensive. The metallic components are also vulnerable to corrosion in the long term. The problems of anchorage systems increase the complexity of using prestressed FRP reinforcement. Thus, it is of great interest to investigate methods that can efficiently apply prestressed FRP reinforcement and meanwhile eliminates the need for mechanical anchorage systems.

Although prestressing FRP laminates contributes to further improvement in the serviceability performance and ultimate capacity of concrete beams, there are limits on the level that the FRP laminates can be pre-tensioned to. One limit of the prestressing level is set in order to avoid over-reinforcing; an excessively prestressed FRP bonded to the soffit of a reinforced concrete (RC) beam might lead to the undesirable failure of FRP even before yielding of steel reinforcement. To optimise the use of prestressed FRP reinforcement, it is important to study the effects of the prestressing level on the structural behaviour and failure mode of FRP-strengthened concrete beams. Numerical simulations based on finite element analysis (FEA) provide a feasible and cost-effective approach to optimisation. However, the difficulty in performing FEA of FRP-strengthened concrete members is to properly model not only the FRP-concrete adhesive bond but also the initiation and development of cracks in concrete. Modelling the failure of bonded FRP induced by critical cracks highly involves nonlinearity and stiffness degradation in the definition of material and interfacial properties, which increase the modelling complexity, convergence difficulties, and computational costs. Therefore, it is worth developing a modelling strategy that allows practical applications of nonlinear FEA in a cost-efficient way to optimise FRP-strengthening of RC beams.

The strengthening efficiency when using prestressed FRP reinforcement might also be limited by the compressive capacity of concrete. Thus, an increase in the prestressing level or amount of the applied FRP reinforcement may not increase the flexural capacity of strengthened RC beams. Instead, the utility of the prestressed FRP reinforcement can decrease due to the flexural failure becoming governed by concrete crushing in the compressive zone of the beam. To eliminate this limit and further improve the flexural capacity by using prestressed-FRP-strengthening, it was proposed in the research project SUREBRIGE [25], which was part of the work in the current thesis, to use glass-FRP (GFRP) panels in combination with externally bonded prestressed CFRP plates for strengthening RC bridge superstructures. The GFRP panel is installed on top of the existing concrete deck acting as compressive reinforcement, and the prestressed CFRP plates were externally bonded to the soffit of the girder (or deck) as tensile reinforcement. This hybrid FRP strengthening system was studied in the current work to investigate its efficiency and robustness in strengthening the deck and girder system of RC bridge superstructures.

In the past four decades, most research on the use of externally bonded FRP was conducted on sound concrete members without considering common deterioration problems of existing RC structures, the major one being corrosion of steel reinforcement. However, the routine use of bonded FRP might not be effective for strengthening deteriorated concrete. More specifically, corrosion-induced cracks in deteriorated concrete members tend to significantly undermine the efficiency of bonded FRP laminates in flexural strengthening [26]. Recent experimental studies [27,28] showed that merely using bonded FRP laminates for flexural strengthening could not effectively enhance the capacity of concrete beams with corroded steel reinforcement, due to premature failure initiated by the separation of concrete cover (with corrosion-induced cracks) and accompanied with a low utilisation ratio of the FRP reinforcement. For the strengthening of existing concrete members, it is important to consider the effects of deterioration and further explore effective strengthening systems using bonded FRP.

1.2 Aim and objectives

This research aims to investigate robust and efficient FRP-strengthening systems to improve the structural capacity of existing RC structures, with a focus on RC bridge superstructures. To achieve this aim, the following objectives were defined in alignment with the aforementioned research gaps:

For sound RC structures

- To study innovative methods to apply prestressed CFRP plates without the need for mechanical anchorage systems and further investigate the efficiency of the applied prestressed CFRP plates in strengthening RC members;
- To develop a practical modelling strategy for performing nonlinear FEA of CFRP-strengthened RC members to optimise the prestressing level of the applied CFRP plates;
- To investigate the robustness and efficiency of the hybrid FRP strengthening system (using GFRP panels complementary with prestressed CFRP plates) for strengthening the superstructure of existing RC bridges;

For deteriorated RC structures with corroded steel reinforcement

- To explore and investigate effective bonded-FRP systems for strengthening deteriorated concrete members with corroded steel reinforcement.

1.3 Methodology

The methodological approaches adopted in this research are illustrated in Figure 1. Even though not reported in this thesis, questionnaires were designed and sent to relevant transport agencies in Sweden, Italy, and the Netherlands at the beginning of the research project SUREBRIDGE [25]. The analysis of collected replies helped to identify the practical problems and demands prioritized by the agencies. Meanwhile, literature studies were conducted to provide state-of-art research and existing solutions in the field of strengthening RC structures with externally bonded FRP composites. Based on the knowledge of current demands and existing techniques, research gaps were identified in the fields of strengthening with externally bonded prestressed FRP and FRP-strengthening of deteriorated RC structures. Accordingly, research objectives were set to bridge the gaps. A series of experimental programmes were designed and conducted to investigate feasible FRP-strengthening systems. Multiple approaches were adopted in the phases of designing, conducting, and evaluating the experiments as shown in Figure 1. Numerical simulations based on FEA were conducted for further evaluation and comparison with experimental results. Based on the evaluation of experimental and numerical results, conclusions and suggestions were summarized in accordance with the aim and objectives of this research.

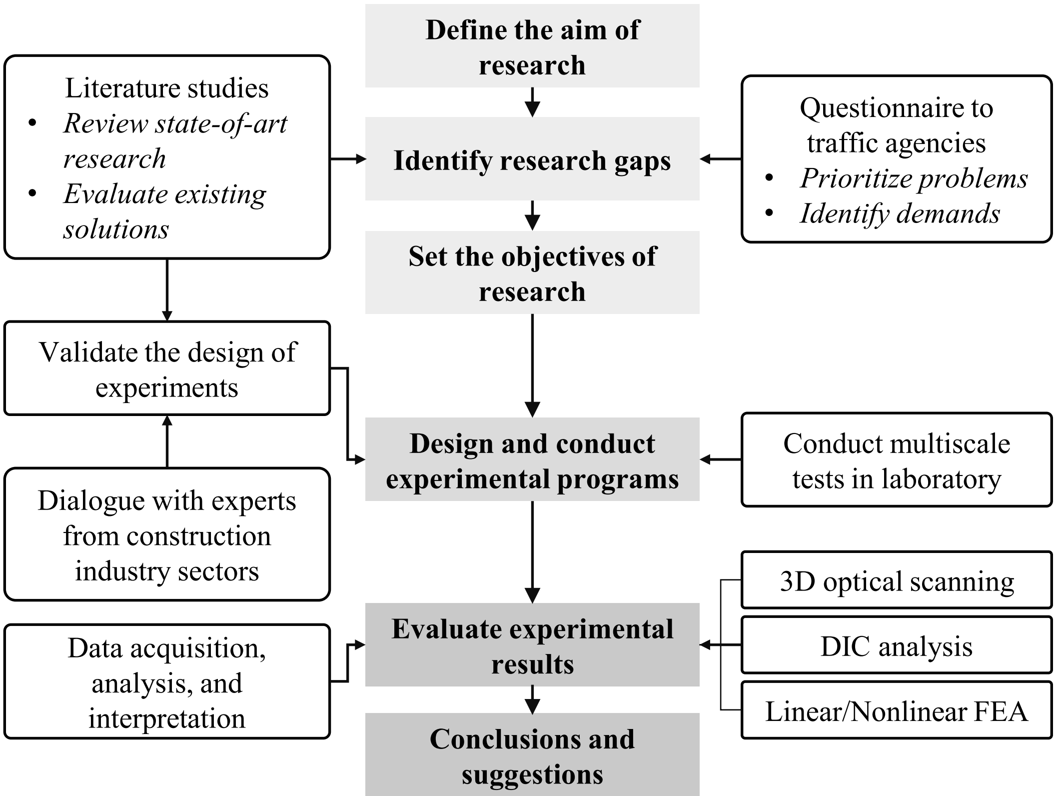

Figure 1. Methodological approaches adopted in the current research.

1.4 Limitations

The limitations of the current work are summarised as:

- The existing reinforced concrete structures in consideration were mainly concrete bridges and their concrete girders and decks as the critical structural components of bridge superstructures.
- Robust and efficient FRP-strengthening techniques were investigated for flexural strengthening of concrete members. Strengthening in shear or axial compression was not the focus of the current work.
- FRP-strengthening systems in the current work were investigated to bridge the gap in the research field of externally bonded FRP techniques. Thus, FRP composites applied in other configurations such as near-surface mounted were not included.

- In the current work, the deterioration of RC structures considers corrosion of steel reinforcement and corrosion-induced cracks in the concrete cover.

1.5 Original features

The original features of the current work are summarised below:

- It was shown in experiments that the stepwise prestressing method could realize the self-anchorage of prestressed CFRP plates on the concrete surface and thus eliminate the need for mechanical anchorage systems.
- The hybrid FRP strengthening system comprising of prestressed CFRP plates and prefabricated GFRP panels was shown to be efficient and robust in improving the flexural stiffness and capacity of RC members.
- The FRP-strengthening system investigated in Paper V was effective to significantly improve the flexural capacity of deteriorated concrete beams, despite high corrosion levels of steel reinforcement and unrepaired concrete cover with corrosion-induced cracks.

1.6 Outline of the thesis

This thesis is comprised of an introductory part and five appended papers. The introductory part consists of four chapters.

Chapter 1 introduces the background, aim, and objectives of the research, and presents the methodology, limitations, and original features of the current work.

Chapter 2 describes the FRP-strengthening systems applied and investigated in the current work.

Chapter 3 provides an overview of the current work regarding the experimental programmes, FEA, and summaries of the appended papers.

Chapter 4 concludes this work and provides suggestions for future research.

2 Externally bonded FRP strengthening systems

2.1 Overview

Since the commence of research on applying FRP to civil infrastructures in the late 1980s [29], FRP composites have been commonly used as externally bonded reinforcement (EBR) in the form of plates, sheets, or strips to strengthen structural RC elements subjected to bending [17], shear[18,16], or axial loading [17,16,18,30]. Several guidelines and recommendations for the design of externally bonded FRP reinforcement have been published worldwide by, e.g., *fib* in Europe [31,32], CNR in Italy [33], Concrete Society in the UK [34], ACI in the United States [35], CSA in Canada [36], JSCE [37] in Japan, and independent researchers [38,39].

The EBR technique is considered to be a cost-efficient alternative to replacing functionally deficient RC members. For flexural strengthening, the EBR can be applied to the soffit of RC members using the so-called wet lay-up method or epoxy adhesive. In the wet lay-up method, fibre fabrics or sheets are saturated in epoxy resin and then bonded to the concrete surfaces to form FRP laminates after curing of the epoxy. Alternatively, it is common to use CFRP plates (i.e. FRP laminates prefabricated by pultrusion method with unidirectional carbon fibres to offer high stiffness and strength) and directly bond to concrete surfaces with epoxy adhesive.

However, the CFRP plates used as EBR tend to debond from concrete surfaces at a low stress level in the plates due to the limited tensile strength of concrete; only 20-30% of the CFRP tensile strength is used when they are applied as ERB for flexural and shear strengthening of RC structural members [40]. To fully utilise the strength of externally bonded CFRP plates, researchers have proposed prestressing them before bonding [21,22]. Compared to the conventional EBR, using prestressed CFRP plates not only increases the utilisation of the CFRP tensile strength but also offers advantages including smaller crack widths, reduced deflection, and improved flexural stiffness and capacity [40,41]. To assure the function of prestressed CFRP plates, it is important to install mechanical anchorage systems at their ends to transfer the prestress force to concrete [23,24].

Although the EBR technique has been widely used for strengthening RC structures, the routine use of FRP as EBR might not be effective for deteriorated RC members. For instance, corrosion-induced cracks in deteriorated concrete members might significantly undermine the efficiency of using externally bonded FRP reinforcement for flexural strengthening [26,27], due to the spalling of concrete cover accompanied by relatively low utilisation of the FRP. The research on effective EBR systems for strengthening deteriorated RC structures started to gain attention in the late 2000s [26,27,42–51].

In the aforementioned fields of EBR using prestressed CFRP plates and EBR strengthening systems for deteriorated RC members, research is needed to fill in the gaps as identified and motivated in Section 1.1. In the current work, three strengthening systems based on externally bonded FRP reinforcement were investigated to evaluate their efficiency in strengthening RC members subjected to bending:

- Prestressed CFRP plates were used as externally bonded reinforcement for flexural strengthening of RC beams. The prestressed CFRP plate was applied using the so-called stepwise prestressing method to realise the self-anchorage of the plate on the concrete beam and thus eliminate the need for conventional mechanical anchors. The application of self-anchored prestressed CFRP plates is introduced in Section 2.2;

- The combined use of prestressed CFRP plates as tensile reinforcement and GFRP panels as compressive reinforcement was studied for strengthening RC members in bending. This hybrid FRP strengthening system is described in detail in Section 2.3;
- A hybrid configuration of externally bonded FRP composites was studied to investigate their effectiveness in strengthening deteriorated concrete beams with corroded steel reinforcement. This bonded-FRP system, including externally bonded FRP laminates on the beam soffit and CFRP U-jackets discretely installed along the beam span, is introduced in Section 2.4.

2.2 Self-anchored prestressed CFRP plates

To realise the self-anchorage of prestressed CFRP plates, an innovative method was used in the current work. This method, namely the stepwise prestressing method, was proposed by Haghani et al. [52] at Chalmers University of Technology. In collaboration with the Swedish Transport Administration, they started the development of this method and its prestressing tools for practical applications in 2009. This method was designed for applying prestressed CFRP plates to concrete members and realise the self-anchorage of the prestressed plates without the need for mechanical anchors. It was shown in previous experimental studies [53] that using the stepwise prestressing method could safely anchor a prestressed CFRP plate to a concrete surface given a prestressing level of 33% (of the CFRP tensile capacity). Compared with conventional prestressing methods, the stepwise prestressing method reduced the difficulty and cost of using the prestressed CFRP plates as the installation and maintenance of the mechanical anchorage system were eliminated.

Figure 2.1 compares the stepwise prestressing method with the conventional approach, in terms of axial force and interfacial shear stress along the bonded prestressed CFRP plate, to explain why the end anchorage system is required conventionally but not needed by using the stepwise prestressing method. In the conventional approach, the prestressing force in the CFRP plate tends to transfer to the concrete member over a short length $L_{0.\mathrm{conv}}$ (usually 50-100 mm) at the plate ends. Given the fact that the magnitude of interfacial stresses is linearly proportional to the gradient of the axial force along the bonded plate [54,55], the great force-transfer over this short length $L_{0.\mathrm{conv}}$ gives rise to interfacial stresses (e.g. shear stress in Figure 2.1a) which are several times higher than the strength of concrete and thus likely to trigger the debonding of the CFRP plate from the concrete surface. To prevent premature debonding of the prestressed plate, it is essential to install mechanical anchors at the laminate ends, despite their cumbersome and labour-intensive installation.

Unlike the conventional method, the stepwise prestressing method, using the prestressing tool shown in Figure 2.2, is designed to create a gradually decreasing profile of the axial force towards the ends of the CFRP plate. As illustrated in Figure 2.1b, the decrease of axial force takes place within multiple segments along the bond line over a much longer length $L_{0.\mathrm{step}}$ than $L_{0.\mathrm{conv}}$ of the conventional approach. As a result, the gradient of the axial force and the resulting interfacial shear stress are much smaller than those of the conventionally prestressed plate. Theoretically, by manipulating the gradient of the axial force in the CFRP plate, these interfacial stresses over $L_{0.\mathrm{step}}$ can be reduced below a certain level and thus transferred safely via the CFRP-to-concrete adhesive bond to concrete without the need for the mechanical anchors.

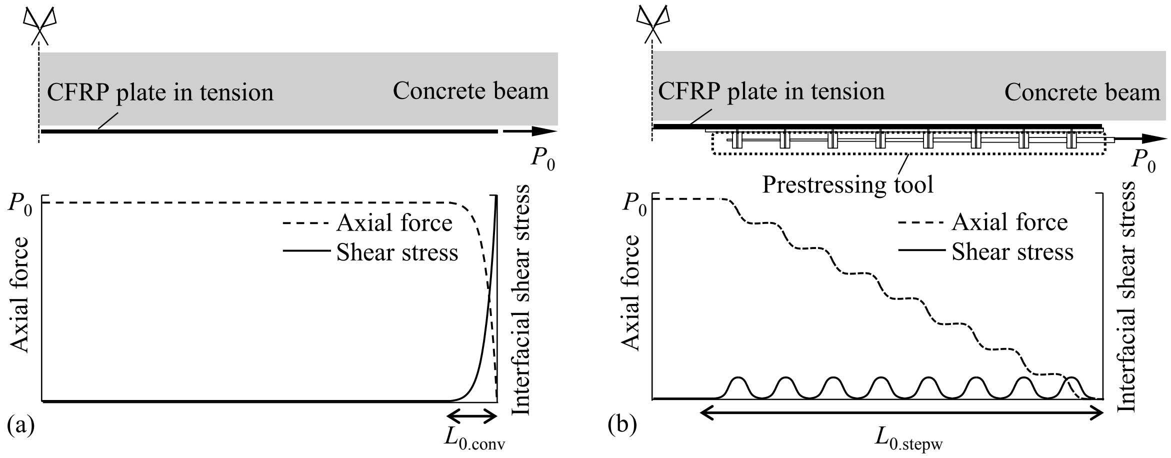

Figure 2.1. (a) Stepwise prestressing method compared with (b) the conventional approach for applying prestressed CFRP plates regarding axial force and interfacial shear stress along the bonded plate [56].

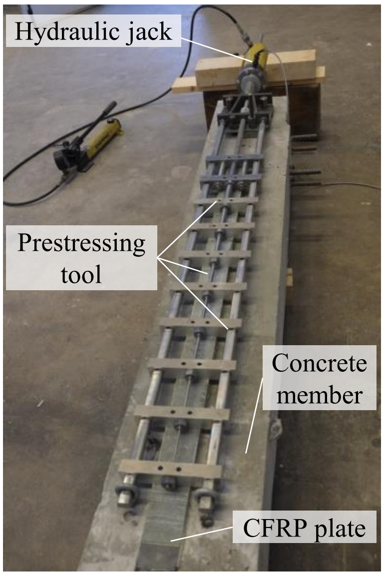

Figure 2.2. The prestressing tool of the stepwise prestressing method used to apply prestressed CFRP plates to a concrete member [53].

In the current work, this stepwise prestressing method was studied and used to apply self-anchored prestressed CFRP plates as EBR for flexural strengthening of RC beams. **Paper I** comprehensively studied this prestressing method regarding its principle, prestressing system and tools, operational procedure, implementation to RC beam specimens, and analyses of interfacial stresses along the self-anchored prestressed CFRP plate. The applied self-anchored prestressed CFRP plate was further investigated in experimental and numerical approaches regarding its efficiency in flexural strengthening of RC beams. This is included in **Paper II** and **Paper III**, as described in Section 3.2.

2.3 Hybrid FRP strengthening system for RC bridge superstructures

As introduced in Section 1.1, the strengthening efficiency of prestressed CFRP plates might be limited by crushing of the concrete in the compression zone of a flexural RC member. To further develop the potential of using prestressed CFRP plates, it was originally proposed in the research project SUREBRIDGE [25] (one of the projects funding the current research) to add prefabricated GFRP panels acting as external compressive reinforcement on the top of RC members. The combined use of prestressed CFRP plates and GFRP panels was proposed as an FRP-solution for strengthening the superstructure of existing concrete bridges. Figure 2.3 demonstrates this hybrid FRP strengthening system applied to the deck and girder of a concrete bridge. In the bridge superstructure subjected to bending, prestressed CFRP plates are applied to the soffit of concrete girders as externally bonded tensile reinforcement. The aforementioned stepwise prestressing method can be used to realise the self-anchorage of the CFRP plates without mechanical anchors. Prefabricated GFRP panels are installed on the top of the old concrete deck. The GFRP panels act as compressive reinforcement and take most of the compressive force originally at the top of the concrete deck.

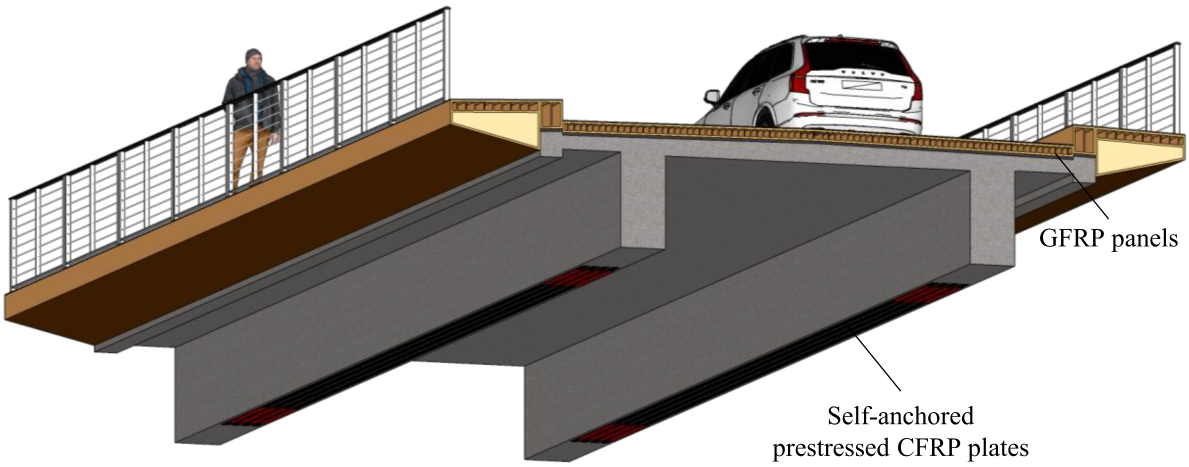

Figure 2.3. Hybrid FRP strengthening system using self-anchored prestressed CFRP plates and GFRP panels for strengthening the superstructure of existing concrete bridges.

Using the GFRP panels complementary with the applied prestressed CFRP plates had the potential to provide the following benefits:

- Significantly improving the flexural stiffness and capacity of RC members owing to the synergy between the prestressed CFRP plates in tension and GFRP panels subjected to compression;
- Removing the limit of the prestressing level or amount of the applied prestressed CFRP plates by protecting the concrete on the compressive side from crushing;
- Providing the opportunity for geometrical upgrading of the bridge deck. The prefabricated GFRP panels can be supplied in tailored dimensions to meet the demand for geometrical expansion, such as widening the bridge deck by adding pedestrian lanes as shown in Figure 2.3;

The hybrid FRP strengthening system was studied in the current work to investigate its efficiency in strengthening RC beams with a T-shaped cross-section. Based on the experimental investigation, the aforementioned benefits were evaluated with a focus on the improvement in flexural performance and the protection from concrete crushing. As reported in **Paper IV**, this hybrid strengthening system was also referred to as SUREBRIDGE solution.

2.4 Bonded-FRP system for deteriorated RC beams

Corrosion of steel reinforcement is the most common deterioration mechanism in concrete bridges during service life. Corrosion-induced damage entails not only the reduction in effective cross-sectional area of steel rebars but also cracking in the concrete cover due to the volume expansion of corroding steel bars. The corrosion-induced cracks along the steel reinforcement impair the surrounding concrete cover and weaken the bond between the steel and concrete. These corrosion-induced damages might render externally bonded FRP reinforcement ineffective in strengthening concrete members suffering from moderate to severe corrosion of steel reinforcement [26,42,50]. Previous experimental studies showed that merely using bonded FRP laminates on the soffit of a deteriorated concrete beam could not effectively enhance its flexural capacity due to the separation of concrete cover that was previously damaged by corrosion-induced cracks [27,28].

To assure the utilisation of externally bonded FRP reinforcement, mortar patch repair is commonly used to remove the damaged concrete cover before bonding FRP composites to the beam soffit. However, patch repair intervention might not be feasible for deficient structures vulnerable to the removal of old concrete. Patch repair in the field might also be discouraged concerning its labour-intensive work, high environmental impacts (e.g. dust, vibration, and noise), and social costs due to traffic closure. A few experimental studies conducted recently [26,27] indicated that, before bonding the FRP laminates, a patch repair to deteriorated concrete cover might not be necessary for increasing structural capacity. From the perspective of infrastructure owners, eliminating the need for costly patch repairs is of great interest, especially in projects only requiring a short-term extension of service life. Therefore, it is necessary to further explore effective bonded-FRP systems that can be applied to highly deteriorated RC beams without repairing damaged concrete cover.

In the current work, a hybrid configuration of externally bonded FRP was investigated for strengthening deteriorated RC beams with corroded steel reinforcement and unrepaired corrosion-damaged concrete cover. As shown in Figure 2.4, this bonded-FRP system consisted of externally bonded FRP reinforcement on the beam soffit for flexural strengthening and CFRP U-jackets discretely installed along the span to provide transverse confinement of beam sections. To optimise the use of U-jackets, those near the end of bonded FRP reinforcement were installed with an inclination of 45° [57]. The experimental study of this bonded-FRP system is reported in **Paper V**.

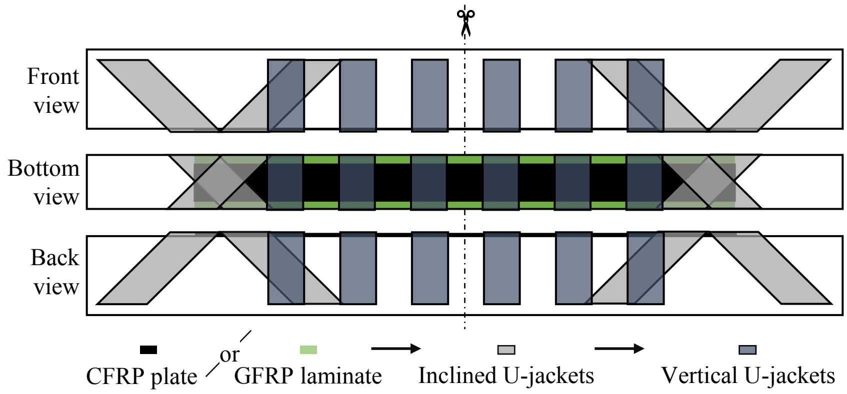

Figure 2.4. Bonded-FRP system for strengthening deteriorated concrete beams without repairing corrosion-damaged concrete cover.

3 Experimental and numerical studies in the current work

3.1 Overview

To meet the research objectives, three experimental programmes were conducted in the current work to investigate the FRP-strengthening systems introduced in Section 2. Based on the experimental studies, numerical simulations using finite element analyses (FEA) were also conducted for comparison, further evaluation, and optimisation. The experiments, FEA, and evaluation of the experimental and numerical results were reported in the appended papers (**Paper I-V**). An overview of the current work is shown in Figure 3.1.

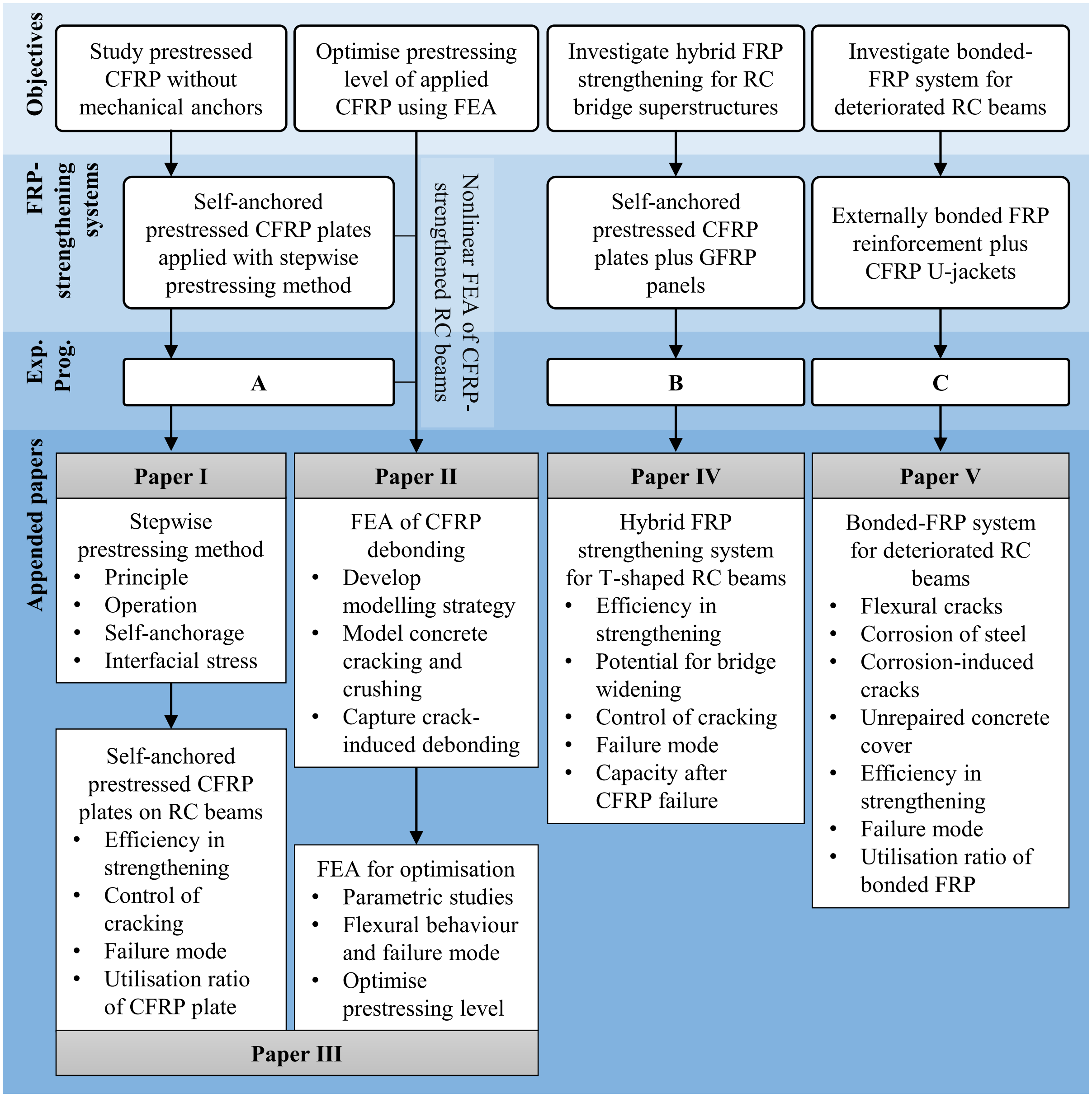

Figure 3.1. Overview of the current work including objectives (an abbreviated version of the objectives described in Section 1.2), FRP-strengthening systems, experimental programmes, and topics analysed in the appended papers.

3.2 Self-anchored prestressed CFRP plates and FEA for optimisation

3.2.1 Description of experimental programme A

Experimental programme A was conducted to a) study the stepwise prestressing method for applying self-anchored prestressed CFRP plates in **Paper I**, b) investigate the efficiency of the self-anchored prestressed plates in strengthening RC beams in **Paper III**, and c) provide experimental specimens and data that was used to validate the finite element modelling strategy developed in **Paper II.** Further, FEA for optimising the applied prestressed CFRP plate was performed in **Paper III**.

Experimental programme A included three RC beams: one reference and two strengthened with different techniques. The first beam (B1) was not strengthened and served as a reference. The second beam (B2) was externally bonded with a passive (non-prestressed) CFRP plate. The third beam (B3) was first pre-loaded in four-point bending under a load of 30 kN (equivalent to 50% of the theoretical yielding load) to induce pre-cracks. After removing the pre-loading, the stepwise prestressing method (introduced in Section 2.2) was used to apply a self-anchored prestressed CFRP plate to specimen B3 without using mechanical anchors. A prestressing level of 27% (of the CFRP tensile capacity) was induced in the CFRP plate. The stepwise prestressing method and its implementation to specimen B3 are comprehensively discussed in **Paper I**.

The prepared specimens were subjected to four-point bending tests as shown in Figure 3.2a. During the tests, midspan deflection, axial strain in CFRP plates, and crack widths were measured to study the flexural behaviour of the specimens. Linear variable differential transducers (LVDTs) were used to obtain the net deflection at midspan. Strain gauges were installed on the CFRP plates to measure axial strains, e.g. 19 strain gauges on the CFRP plate of specimen B3 to monitor the development of strains in the prestressing and loading phases (Figure 3.2b). A handheld digital microscope was used to measure crack widths at the height of tensile reinforcement at multiple load levels. More details of the flexural tests are described in **Paper III**.

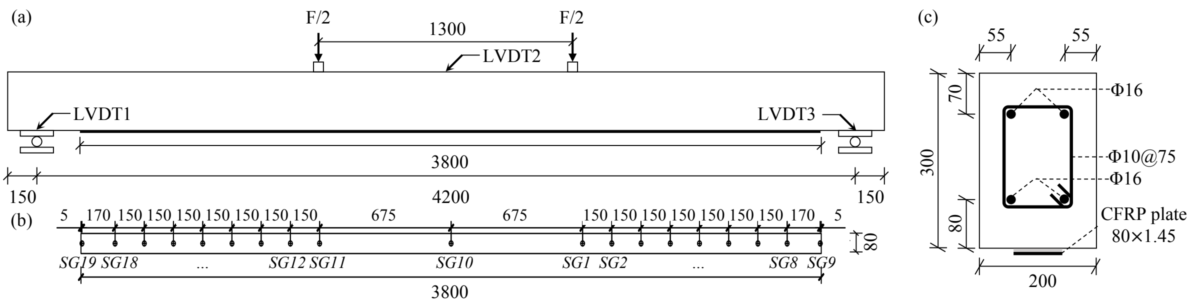

Figure 3.2. (a) Test set-up for specimens in experimental programme A, subjected to four-point bending; (b) bottom view of the self-anchored prestressed CFRP plate on specimen B3 with 19 strain gauges installed along its length; (c) cross-sectional dimensions of the RC beams with bonded CFRP plate (applied to B2 and B3 only).

3.2.2 Summary of Paper I

Paper I investigated the stepwise prestressing method for applying prestressed CFRP plates to concrete beams without the need for mechanical anchors. The stepwise prestressing method proposed by Haghani et al. [52] was comprehensively studied herein regarding its principle, prestressing system and tools, operational procedure, and implementation to specimen B3. Figure 3.3 shows how the prestressing system is used to apply a prestressed CFRP plate to the soffit of an RC beam.

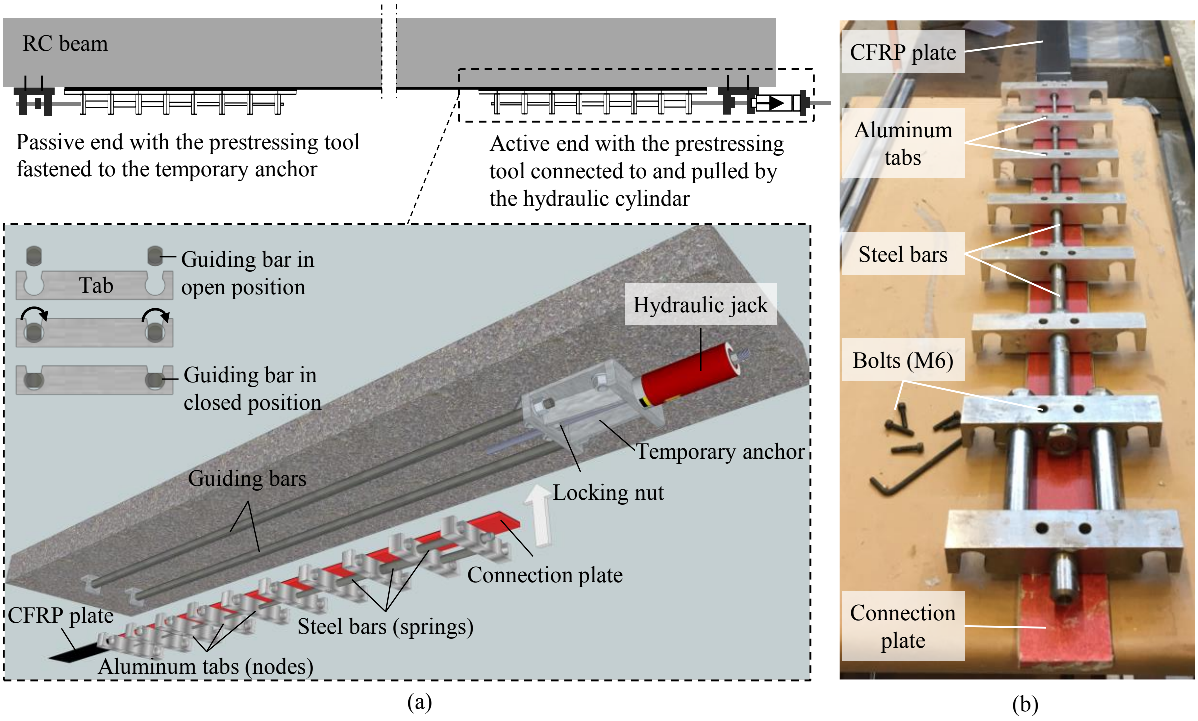

Figure 3.3. (a) Apply a prestressed CFRP plate to the soffit of an RC beam using the stepwise prestressing method; (b) mechanical prestressing tool as the critical component of the prestressing system.

In the prestressing phase, the maximum force from the hydraulic jack reached 100 kN. It resulted in a maximum tensile strain of 4.0‰ at midspan of the CFRP plate, corresponding to a prestressing level of 31% (of the CFRP tensile capacity). After curing of the adhesive and removal of the prestressing system, the tensile strain at midspan dropped to 3.5‰ equivalent to a prestressing level of 27%. Figure 3.4 shows the prestressed CFRP plate safely anchored on the surface of specimen B3.

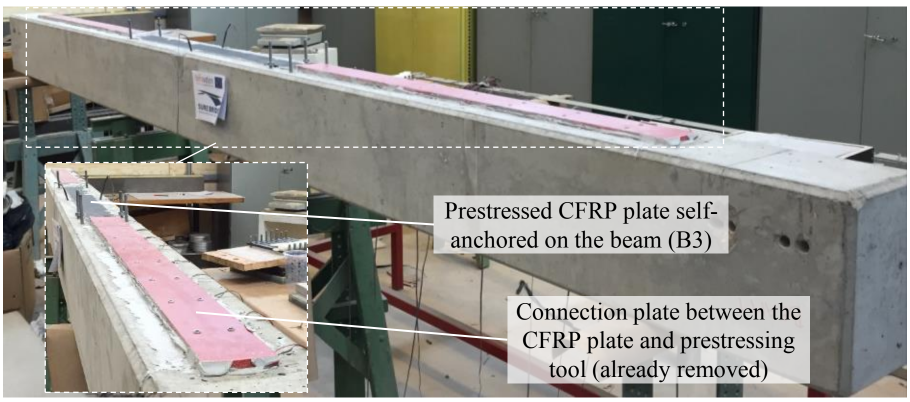

Figure 3.4. Self-anchored prestressed CFRP plate on the concrete beam (specimen B3) after removal of the prestressing system.

Numerical simulations based on FEA were conducted to investigate the axial force distribution in the self-anchored CFRP plate and interfacial stresses along the bond line. Figure 3.5 compares the stepwise prestressing method with the conventional prestressing approach in terms of the axial strain in the CFRP plate, shear stress in the adhesive layer, and shear stress 1-mm-beneath the concrete surface. The comparison of these results revealed the difference in the force-transfer from the bonded prestressed CFRP plate via the adhesive layer to the concrete beam. In the stepwise prestressed method, the axial force in the prestressed plate decreased towards the plate end over a longer distance (i.e. anchorage length) than that of the conventional approach. As a result, the critical interfacial shear stress along the bond line, linearly proportional to the gradient of the axial force in the plate, was significantly lower in the stepwise prestressing method. As shown in Figure 3.5, the peak shear stresses at 1-mm-beneath the concrete could reach 20 MPa at the end of the conventionally applied prestressed CFRP plate but was less than 0.9 MPa when using the stepwise prestressing method. Compared with these peak stresses, the strength of the CFRP-to-concrete bond (estimated at 5.7 MPa according to [13]) was sufficient to assure the safe self-anchorage of the prestressed plate in specimen B3.

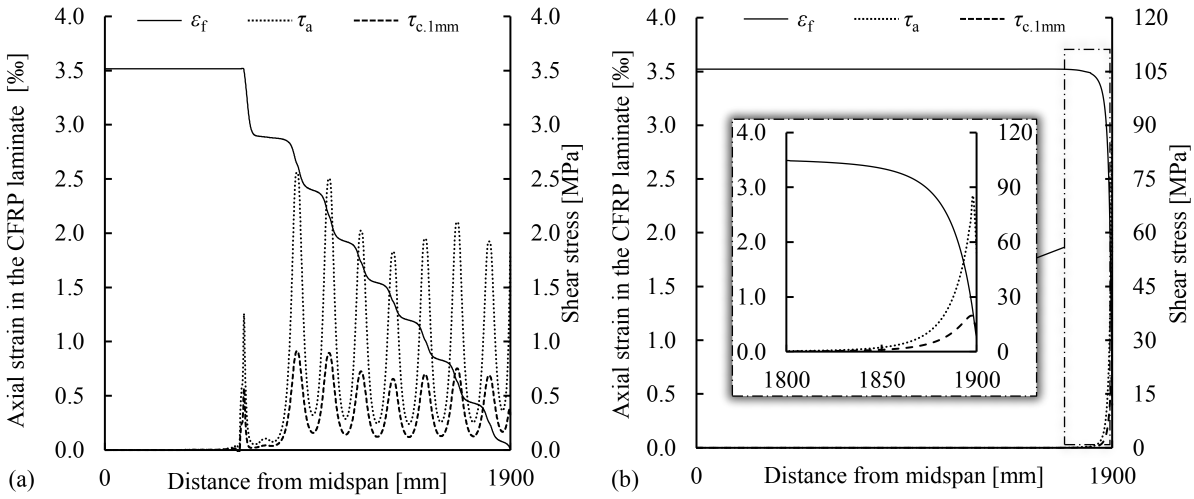

Figure 3.5. Comparing (a) stepwise prestressing method with (b) conventional prestressing approach regarding axial strain in the prestressed CFRP plate, shear stress in the adhesive layer, and shear stress 1-mm-beneath the concrete surface; note the different scales on the y-axes for shear stress.

3.2.3 Summary of Paper II

In **Paper II**, a practical modelling strategy was developed to conduct nonlinear FEA of RC beams and beams strengthened with externally bonded CFRP plates. The nonlinear FEA was conducted in software package ABAQUS/CAE 6.14 [58]. To deliver reliable simulation of flexural cracks, concrete crushing (in specimen B1), and crack-induced CFRP debonding (in specimens B2), the modelling strategy was developed systematically in **Paper II** to cope with the critical issues associated with nonlinear modelling of reinforced concrete and CFRP-to-concrete adhesive joint, such as:

- defining nonlinear behaviour of concrete in tension and compression;
- assigning bond-slip between concrete and steel reinforcement;
- capturing crack-induced CFRP debonding accompanied by the damage evolution of adhesive in the CFRP-to-concrete bond;
- Overcoming convergence difficulty in the static analysis procedure.

The concrete damage plasticity (CDP) model in Abaqus [58] was adopted to model concrete in the RC beams. For concrete tensile behaviour, the smeared crack method was adopted to model a crack as equivalent strain over a crack band. To avoid the sensitivity of FEA results to the mesh size, the width of crack bands was properly determined to consider the topology of concrete elements and orientation of crack bands. More details of the crack band width and mesh sensitivity study are described in **Paper II**.

The concrete compressive behaviour was defined based on the constitutive relationship from Model Codes [59,60]. The post-peak softening branch was properly modified to consider strain localisation in critical crushing zones over L_{cr} (Figure 3.6). The study of three compressive constitutive models of concrete in the current FEA evidenced that the difference in post-peak softening branches significantly affected the simulated flexural responses of RC beams in the ultimate state associated with concrete crushing. Thus, modifying the softening behaviour with properly assumed L_{cr} is critical to a) accurately modelling the flexural failure of RC beams governed by concrete crushing or b) predicting the failure of CFRP-strengthened beams first initiated by concrete crushing or CFRP debonding. In **Paper II**, an iterative procedure was proposed to identify the size of L_{cr} critical to the modification of post-peak behaviour. With the decrease in the assumed size of L_{cr} from 200 to 40 mm, the modified post-peak behaviour of compressive concrete descended at a slower rate (Figure 3.7a), the concrete crushing in the simulated reference beam occurred at a larger midspan deflection (Figure 3.7b), and the size of the concrete crushing zones in the analyses increased from approximately 50 to 160 mm (Figure 3.7d). Based on the iterative study of L_{cr} summarised in Figure 3.7(c), the size of L_{cr} for the beams tested in experimental programme A was determined as 100 mm, as it could be verified by the actual size of the crushing zone in the analyses.

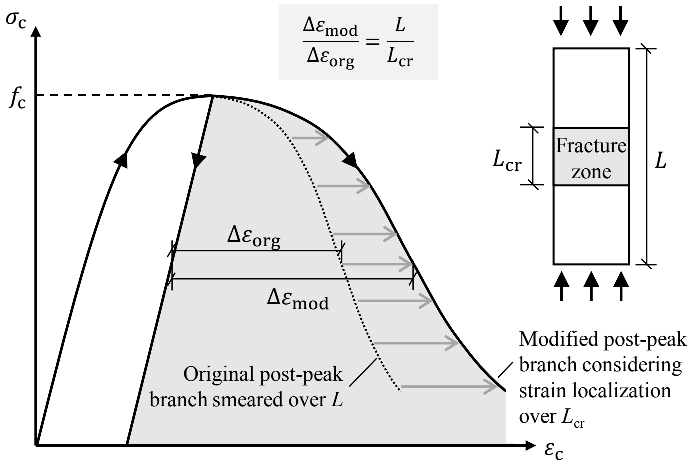

Figure 3.6. Modification of the post-peak softening branch to consider strain localisation in the fracture (crushing) zone.

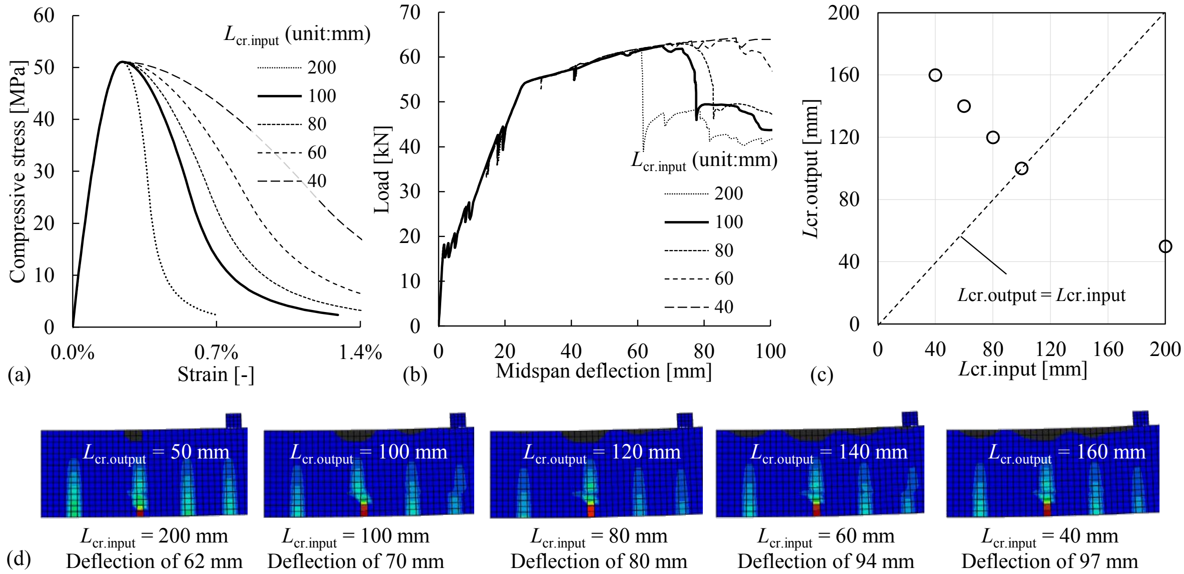

Figure 3.7. (a) Concrete compressive behaviour based on the Model Code relation with the modified post-peak strain-softening branches given different $L_{cr.input}$ values ranging from 40–200 mm; (b) simulated load-deflection relations of the reference beam (B1) corresponding to each value of $L_{cr.input}$; (c) comparison of the assumed $L_{cr.input}$ and the observed size of the critical crushing zone $L_{cr.output}$ for each FE analysis; (d) contour plot of the beam models within the constant-moment region for visualizing the crushing zones and evaluating $L_{cr.output}$ given different values of $L_{cr.input}$.

To correctly describe crack-induced debonding, it was found important to simulate both the crack openings and the CFRP-to-concrete bond accurately. Besides the definition of concrete tensile behaviour, the crack widths also highly depend on the bond-slip behaviour assigned between the steel reinforcement and the concrete. Two different methods were investigated to assign bond-slip models and found capable to deliver numerical results of crack pattern and widths comparable with experimental measurements. The bond-slip model in Model Code [60] corresponding to 'good bond condition' was evidenced suitable for the current FEA of tested beams, after comparing with 'perfect' bond assuming no relative slip and the model for 'other bond conditions' in Model Code [60]. For the CFRP-to-concrete bond, cohesive elements were used to model the adhesive bond layer and characterise the nonlinear bond behaviour including damage evolution and stiffness degradation. This approach could visualise the FRP-debonding process by removing fully damaged cohesive elements.

Based on the proposed modelling strategy, FEA of specimen B1 (reference RC beam) and specimen B2 (RC beam strengthened with a passive CFRP plate) were conducted. The results of the FEA were compared with the experimental measurements in terms of flexural behaviour, crack widths, and failure modes of concrete crushing (in B1) and CFRP debonding (in B2). The comparison showed that proper modelling of cracks in the FEA was essential for reliable prediction of CFRP debonding shown in Figure 3.8.

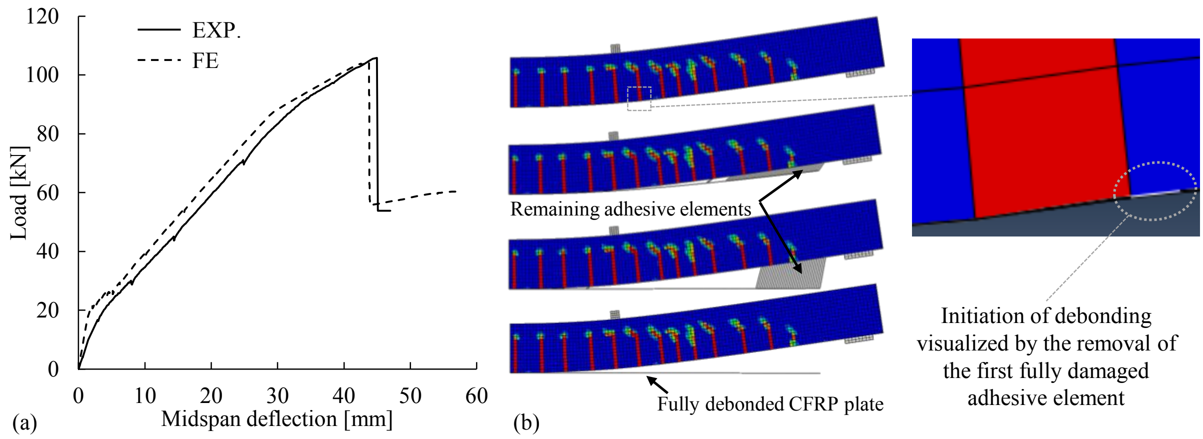

Figure 3.8. (a) Comparison of the flexural responses between experimental measurements (EXP) and FEA results (FE); (b) crack-induced debonding of CFRP plate visualised in FEA of specimen B2 (RC beam strengthened with a passive CFRP plate).

Besides the reliability of results, the developed modelling strategy also gave priority to the cost-efficiency in practical engineering applications. To reduce the complexity of modelling, the models were solved in static analysis procedure rather than dynamic implicit analysis to avoid the complex definition of parameters, such as period of the fundamental vibration mode, viscous damping ratio, loading time, and time increment size. To overcome the convergence difficulty commonly found in static analysis of nonlinear reinforced concrete problems, viscoplastic regularisation was introduced to reduce the computation time effectively.

Based on the modelling strategy in **Paper II**, the FEA could deliver reliable simulations of crack-induced CFRP debonding in CFRP-strengthened RC beams, which served as the foundation for optimising the use of prestressed CFRP plate in **Paper III.**

3.2.4 Summary of Paper III

In **Paper III**, the applied self-anchored prestressed CFRP plate was further investigated regarding its efficiency in flexural strengthening. The flexural behaviour of the specimens in experimental programme A was analysed in terms of load-deflection curves, crack widths, failure modes, and ultimate utilisation ratio of CFRP plates. Besides the evaluation of experimental results, FEA was also conducted based on the modelling strategy in **Paper II** for an optimisation study of the applied prestressed CFRP plate.

Load-deflection curves in Figure 3.9 show that using the self-anchored prestressed CFRP plate (in specimen B3) could further enhance the load-carrying capacity compared with that of specimen B2 strengthened with a passive CFRP plate. The ultimate capacity of B3 was 126% and 39% higher, respectively, than that of reference specimen B1 and specimen B2.

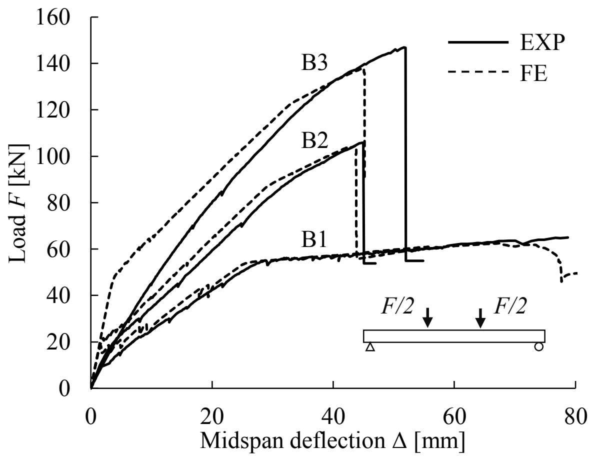

Figure 3.9. Flexural behaviour of specimens subjected to four-point bending tests in experimental programme A; load-deflection curves according to experimental measures (EXP) and FE analyses (FE); B1: reference beam, B2: beam strengthened with a passive CFRP plate, B3: beam strengthened with a self-anchored prestressed CFRP plate.

Although both specimens B2 and B3 exhibited debonding of the CFRP plates, the utilisation ratio of the self-anchored prestressed CFRP plate in B3 was much higher than that of the passive CFRP plate in B2. Figure 3.10 shows the development of axial strain measured by strain gauges at midspan of the CFRP plates in B2 and B3. The maximum tensile strain in the passive CFRP plate was estimated at 5.9‰ in B2, equivalent to a utilisation ratio of 47%. In specimen B3, although the prestressed CFRP plate was self-anchored without mechanical anchors, the maximum tensile strain of the CFRP plate reached 10.3‰ at debonding, corresponding to a utilisation ratio as high as 81%.

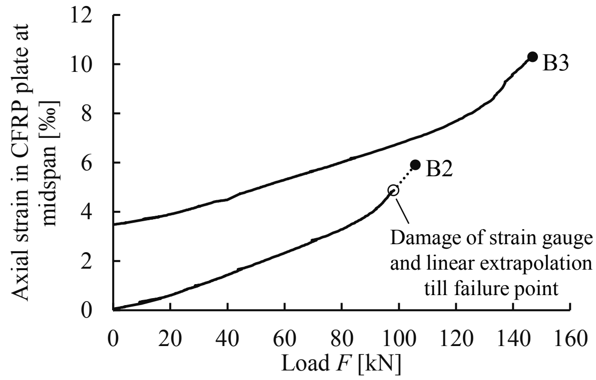

Figure 3.10. Development of the axial strain measured by strain gauges at midspan of the CFRP plates in specimens B2 and B3 with the increase of external load

To optimise the applied prestressed CFRP plate, specimen B3 was modelled and parametric studies were conducted in FEA to investigate the effects of prestressing level and stiffness of CFRP plates on the flexural behaviour and failure mode of the strengthened beam. As shown in Figure 3.11, the ultimate load-carrying capacity rose with increasing prestressing level up to 40%, and the failure was initiated by crack-induced debonding of the CFRP plate. However, when the prestressing level reached 50%, debonding of the CFRP took place earlier than yielding of steel reinforcement and thus led to a decrease in both load-carrying and deformation capacities. The results of FEA indicated that an optimal choice of the prestressing level was

40% for the CFRP plate applied to specimen B3 in terms of obtaining the highest load-carrying capacity.

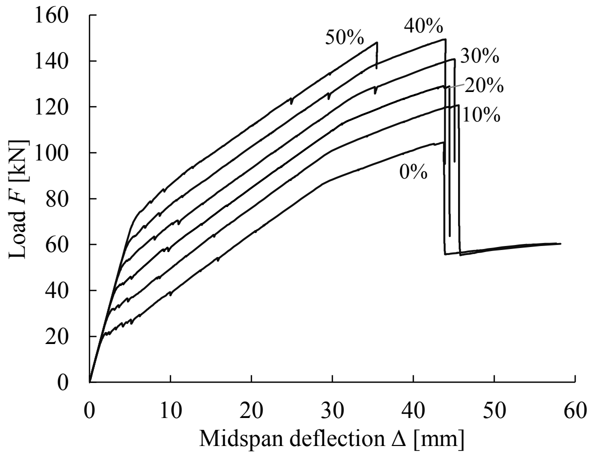

Figure 3.11. Parametric study of prestressing levels from 0-50%; load-deflection curves of CFRP-strengthened RC beams based on the FEA of specimen B3.

3.3 Hybrid FRP strengthening system for RC bridge superstructures

3.3.1 Description of experimental programme B

Experimental programme B was designed to investigate the efficiency of the hybrid FRP-strengthening system using prestressed CFRP plates in combination with GFRP panels in strengthening the superstructure of RC bridges (described in Section 2.4). In experimental programme B, four RC beams were cast with a T-shaped cross-section, see Figure 3.12a and Table 1. The T-beams were designed to represent the deck and girder (i.e. beam-slab) system of RC bridge superstructures.

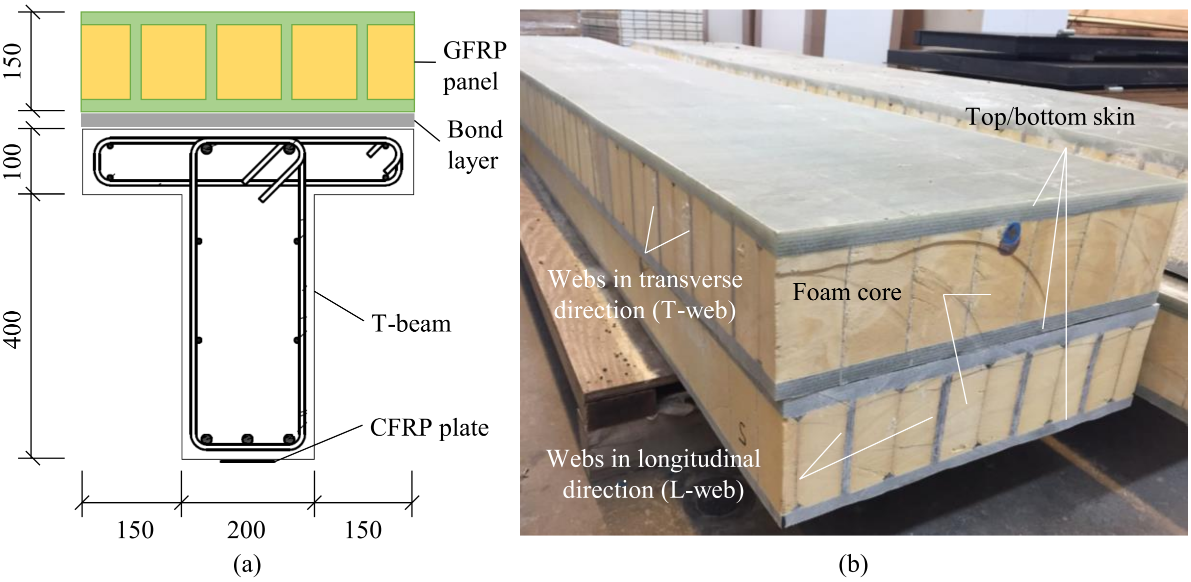

Figure 3.12. (a) Cross-sectional dimensions of the T-beam strengthened with self-anchored prestressed CFRP plate and GFRP panel; (b) Two configurations of GFRP panels with webs in the transverse direction (T-web panel) and webs in the longitudinal direction (L-web panel).

These T-beams were prepared for four-point bending tests to investigate the flexural responses regarding cracking load, flexural stiffness, crack widths, ultimate capacity, and failure mode. To be distinguished from the specimens in experimental programme A, the four specimens in experimental programme B are referred to as TB1-TB4 in the thesis, whereas they are named B1-B4 in the appended **Paper IV**.

Table 1. Specimens in experimental programme B.

Specimens[a]	Prestressed CFRP plate	GFRP panel	Bond layer
TB1	N.A.	N.A.	N.A.
TB2	25%[b]	L-web[c]	10-mm-thick expoxy adhesive
TB3	25%[b]	L-web[c]	30-mm-thick mortar
TB4	29%[b]	T-web[c]	30-mm-thick mortar

[a]Specimens TB1-TB4 are referred to as B1-B4 in the appended Paper IV; [b]Prestressing level in the CFRP plate: the ratio of the induced prestress to the CFRP tensile strength; [c]GFRP panel with webs oriented in the longitudinal/span direction (L-web) or webs in the transverse direction (T-web).

As summarised in Table 1, specimen TB1 was not strengthened and served as a reference. The other three specimens TB2-TB4 were strengthened with a self-anchored prestressed CFRP plate on the beam soffit and a prefabricated GFRP panel on the top of the beam flange. The differences among TB2-TB4 were in the prestressing level of applied CFRP plates, the configuration of GFRP panels, and the bond layer between the GFRP panels and T-beams.

The self-anchored prestressed CFRP plates were applied with the stepwise prestressing method, same as experimental programme A. Although the same prestressing level was designed, the prestressing level in specimen TB4 (29%) was higher in practice than that (25%) of specimens TB2 and TB3. GFRP panels with different configurations of webs are shown in Figure 3.12b: panel with webs oriented in the longitudinal direction (L-web panel) or webs in the transverse direction (T-web panel). Using the L-web panel could obtain higher bending stiffness and structural capacity, whereas the T-web enables a panel wider than the concrete deck and thus provides the chance of widening the original deck. The panels were bonded with two different materials: using 10-mm-thick epoxy adhesive in TB2 and 30-mm-thick low-shrinkage mortar in TB3 and TB4.

3.3.2 Summary of Paper IV

Paper IV introduced the four-point bending tests in experimental programme B and evaluated the strengthening efficiency of the hybrid strengthening system using prestressed CFRP plate and GFRP panel. The contributions made by the hybrid strengthening system were discussed based on the flexural behaviours of the tested specimens shown in Figure 3.13.

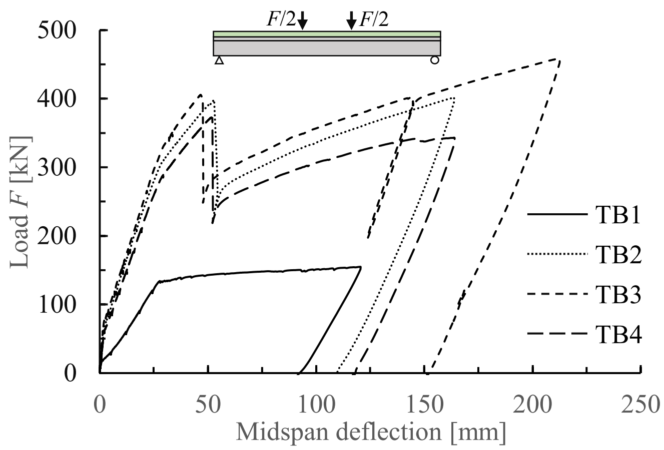

Figure 3.13. Load-deflection curves of specimens TB1-TB4 (see Table 1) subjected to four-point bending tests in experimental programme B.

Using the prestressed CFRP plate significantly enhanced the cracking load from 19 kN of reference specimen B1 to 61-75 kN of the strengthened specimens B2-B4. After the cracking stage, the bending stiffness of the strengthened specimens was improved by 82-99% compared with specimen B1. The significant increase in bending stiffness resulted from the bonded CFRP plate and GFRP panel, respectively, acting as the tensile and compressive reinforcement in the RC cross-section subjected to bending.

After yielding of steel reinforcement, debonding of CFRP plates took place in specimens B2-B4 and caused sudden drops in load shown in Figure 3.13. At the moment of debonding, the tensile strains measured at midspan of the CFRP plates were 10.4-10.9‰, equivalent to utilisation ratios of 82-86% (of the CFRP tensile capacity). These utilisation ratios were comparable with that of the self-anchored prestressed CFRP plate (81%) in experimental programme A.

In the 'post-debonding' phase, the strengthened specimens exhibited substantial residual capacities; the load continued to increase even beyond the load at the CFRP debonding. The great residual capacities were obtained owing to the GFRP panel installed on the top of the beam. In the strengthened specimens subjected to bending, the GFRP panel acted as compressive reinforcement and took most of the compressive force. Thus, with the compressive zone shifting to the GFRP panel, concrete crushing at top of the T-beams was prevented, even though the load increased to 350-400 kN in the 'post-debonding phase' (2.3-2.6 time of the maximum load of the reference specimen B1).

Besides the increase of bending stiffness and load-carrying capacity, the hybrid FRP strengthening system also improved the performance of strengthened specimens regarding the control of cracking. Figure 3.14 shows the development of maximum crack widths with the increase of external load. After the strengthening of specimens B2-B4, both the magnitude and gradient of the crack-width growth curve were less than that of the reference specimen B1.

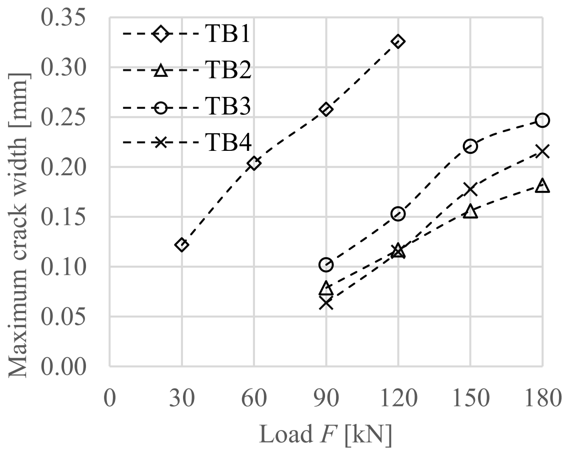

Figure 3.14. Development of the maximum crack width measured in specimens TB1-TB4 at the height of tensile steel reinforcement.

3.4 Bonded-FRP system for deteriorated RC beams

3.4.1 Description of experimental programme C

Experimental programme C was conducted to investigate the efficiency of strengthening methods using bonded FRP composites for deteriorated RC beams with corroded steel reinforcement. The bonded-FRP system (introduced in Section 2.4) was applied to deteriorated beams to investigate its efficiency in flexural strengthening. Ten RC beams were cast and prepared in four groups: RN, DN, DG, and DC, see Table 2. Group RN included two sound beams as references. The other eight beams were pre-cracked and then exposed to identical conditions of accelerated corrosion for 75 days. Figure 3.15 illustrates the set-up for the accelerated corrosion of beams in the laboratory. Average corrosion levels of 17-23% and maximum local corrosion levels in the range of 41-57% were obtained. After the corrosion period, the two beams in group DN were not strengthened, the three beams in group DG were flexurally strengthened with GFRP laminates, and the three beams in group DC were bonded with CFRP plates. In groups DG and DC, the GFRP and CFRP composites were bonded to the soffit of beams without repairing the concrete cover with corrosion-induced cracks; CFRP U-jackets were also installed along the span of the six strengthened beams to provide transverse confinement. The applied bonded-FRP system is shown in Figure 2.5.

Table 2. Specimens in experimental programme C.

Specimen[a]	Flexural strengthening material	Average corrosion level[b] [%] I[d]	Average corrosion level[b] [%] II[d]	Max. local corrosion level[c] [%] I	Max. local corrosion level[c] [%] II
RN1	—	—		—	
RN2	—	—		—	
DN1	—	20	19	50	48
DN2	—	20	21	46	54
DG1	GFRP	22	17	51	40
DG2	GFRP	21	20	43	54
DG3	GFRP	18	23	43	53
DC1	CFRP	23	20	53	55
DC2	CFRP	21	22	49	41
DC3	CFRP	21	22	54	57

[a]The first letter refers to reference (R) or deteriorated (D); the second letter refers to non-strengthened (N), flexurally strengthened with GFRP laminate (G), or flexurally strengthened with CFRP plate (C).
[b]Average corrosion level means the percentage of the mass loss of reinforcement over the corroded length.
[c]Maximum local corrosion level refers to the maximum percentage of the cross-sectional area loss along a steel reinforcement bar.
[d]Corrosion levels are reported separately for the two tensile reinforcement bars, I and II, in each of the beam specimens.

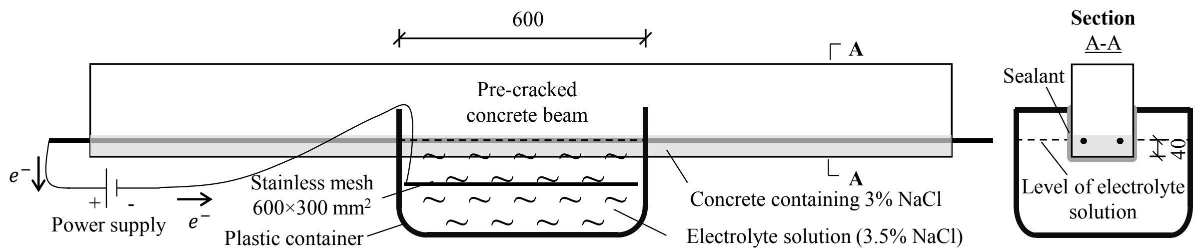

Figure 3.15. Electrical circuit set-up for the accelerated corrosion of pre-cracked concrete beams and side view of the beam in the plastic container.

After preparation, all specimens were subjected to four-point bending tests until failure to study their structural behaviours and failure modes. The test set-up for the specimens is shown in Figure 3.16a. The net-deflection at midspan was monitored using linear variable differential transformers (LVDT) placed at midspan and centre of the two supports. The axial strains in the FRP composites were measured with strain gauges. The side face of beam specimens within the mid-1000 mm zone was monitored by a Digital Image Correlation (DIC) system to obtain and visualise more data in the constant-moment region, such as deformation field and crack propagation.

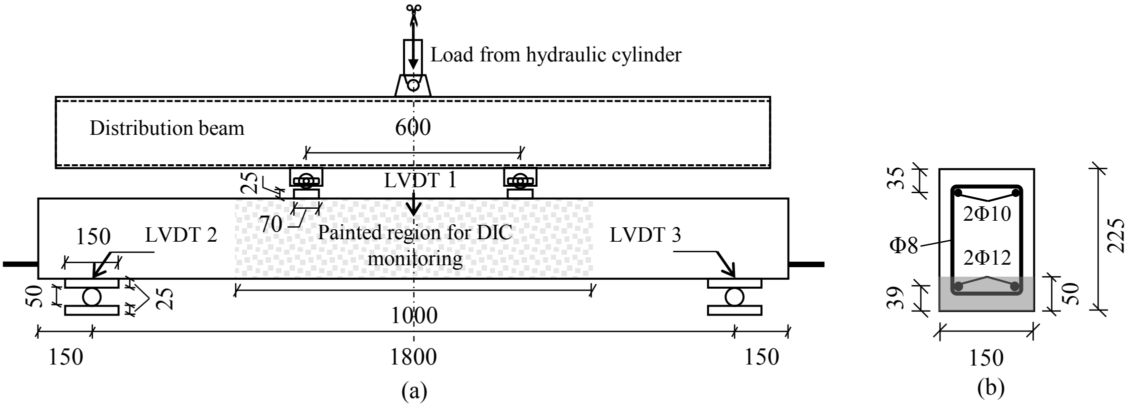

Figure 3.16. (a) Test set-up for specimens in four-point bending tests in experimental programme C; (b) cross-sectional dimensions of specimens.

After the four-point bending tests, the tensile steel reinforcement bars were removed from the eight deteriorated specimens. Both the average and local corrosion levels were measured to quantify the corrosion damage of the steel reinforcement. The average corrosion level referred to the percentage of the mass loss over the corroded length of reinforcement while the local corrosion level was obtained with the 3D scanning technique similarly as [61–63]. The measurements of local corrosion level and corrosion-induced cracks in the eight deteriorated beams are included in Appendix A. More details of experimental programme C are described in Paper V.

3.4.2 Summary of Paper V

In Paper V, experimental programme C was comprehensively reported, including the design of tests, the corrosion and strengthening of specimens, the four-point bending tests, and the evaluation of corrosion damage. The experimental data were analysed to investigate the effects of corrosion damage and the strengthening efficiency of the applied bonded-FRP system.

The flexural behaviours of tested specimens showed that the combined use of externally bonded FRP on beam soffits and CFRP U-jackets along the span was efficient in upgrading the load-carrying capacity of deteriorated concrete beams, despite maximum local corrosion levels of the reinforcement as high as 57%. Figure 3.17a shows the load-deflection curves of the specimens in four-point bending until failure. After strengthening, the ultimate load capacity of the deteriorated specimen DC2 increased to 212 kN, which was 417% and 165% higher, respectively, than that of deteriorated non-strengthened specimens (of group DN) and the reference beams (of group RN).

The bonded-FRP system was effective, even though it was applied directly to the beams without repairing the deteriorated concrete cover. Given the concrete cover with corrosion-induced cracks as wide as 2 mm, the U-jackets effectively suppressed the separation/spalling of the concrete cover. The confinement offered by U-jackets is demonstrated in Figure 3.17b, which compares cracks propagated in the constant-moment region of specimens DN2, DG2, and DC2 at the same midspan deflection. U-jackets installed in specimens DG2 and DC2 effectively suppressed the initiation and development of longitudinal cracks that were noticeably observed in the deteriorated but unstrengthened specimen DN2 even at a much smaller load.

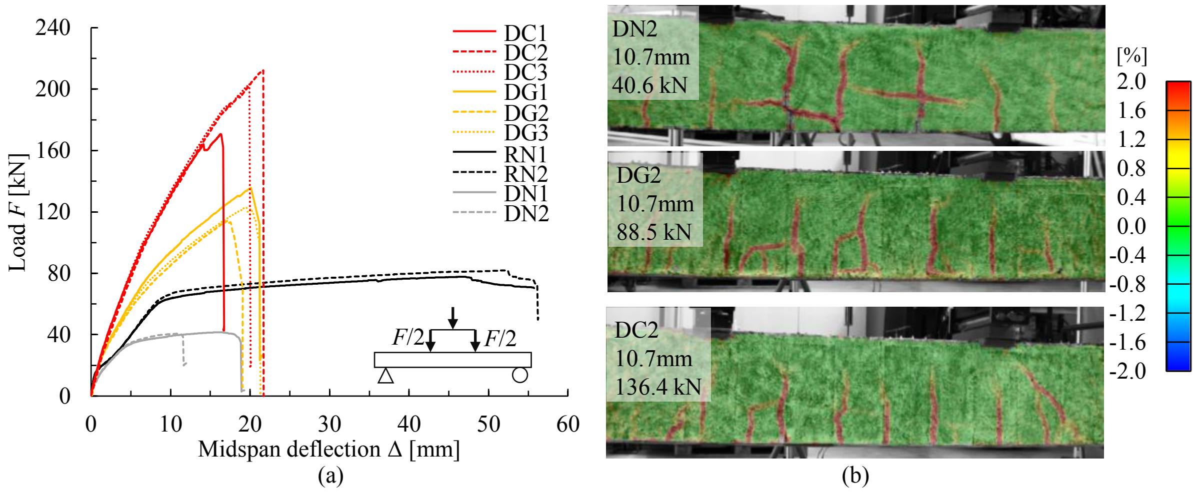

Figure 3.17. (a) Load-deflection curves of all ten specimens (see Table 2) subjected to four-point bending in the experimental programme C; (b) comparison of cracks on the side of specimens (DN2, DG2, and DC2), visualised in the maximum principal strain field monitored by DIC at the same midspan deflection of 10.7 mm.

The suppressed spalling of concrete cover allowed higher utilisation of the bonded FRP on the beam soffits, which was evidenced by rupture of the GFRP laminates in group DG and a utilisation ratio of CFRP plates as high as 64% (of the CFRP plate tensile capacity) in group DC.

The flexural responses of the tested specimens also revealed the importance of evaluating the local corrosion level of steel reinforcement to accurately estimate the effects of corrosion damage on the flexural capacity of deteriorated concrete beams. For instance, the ultimate load of deteriorated beam DN1 was reduced by 48% compared with that of the reference beams. This reduction agrees well with the maximum local corrosion levels of 50% and 48% in the two tensile reinforcement bars of specimen DN1. However, using the average corrosion level of the tensile bars in DN1 (20% and 19%) would overestimate its flexural capacity.

4 Conclusions and future research

4.1 Conclusions

The current work aimed to investigate robust and efficient FRP strengthening techniques to improve the structural capacity of existing RC structures. Three experimental programmes were conducted to investigate the efficiency of applied FRP systems in flexural strengthening of RC members. Besides the experimental studies, numerical simulations using finite element analyses (FEA) were also carried out for comparison, evaluation, and optimisation. Based on the current work, the main conclusions were summarized below following the research objectives.

Self-anchored prestressed CFRP for flexural strengthening
To eliminate the need for mechanical anchorage systems, the stepwise prestressing method was studied to apply prestressed CFRP plates and achieve the self-anchorage of the plates on the concrete surface. Experimental applications in the current work showed that the prestressed CFRP plates were safely anchored to the surface of concrete beams, given prestressing levels of 25-29% (of the CFRP tensile capacity). The FEA also revealed that using the stepwise prestressing method greatly reduced the critical interfacial shear stresses below 0.9 MPa. The reduced interfacial stresses could be safely transferred via the CFRP-to-concrete adhesive bond to the beam without the need for mechanical anchors.

The flexural responses of the strengthened RC beams showed that the self-anchored prestressed CFRP plates were efficient in improving the performance in terms of delaying the onset of cracking, reducing crack width, and increasing flexural stiffness and ultimate load-carrying capacity. The flexural failure of strengthened beams showed that, despite no conventional anchors were installed at the plate ends, the utilization ratios of the CFRP plates were above 80% (in the range of 81-86%) at the moment of debonding.

Optimising the self-anchored prestressed CFRP plates using FEA
To optimise the application of the self-anchored prestressed CFRP plate, a practical finite element modelling strategy was developed in the current work to enable nonlinear FEA of CFRP-strengthened RC beams. Based on the validated modelling strategy, the FEA of specimens in experimental programme A delivered reliable results of flexural cracks and crack-induced CFRP debonding that were comparable to the experimental measurements. Parametric studies were conducted using FEA to investigate the effects of the prestressing level of the applied CFRP plate on the flexural behaviour and failure mode of the strengthened RC beam. The current FEA of specimen B3 showed that there was a threshold of the prestressing level, above which the flexural capacity tended to decrease. In specific, for the self-anchored prestressed CFRP plate applied to specimen B3, an optimal choice of the prestressing level was 40% (of the CFRP tensile capacity) to obtain the highest load-carrying capacity. A higher prestressing level (e.g. 50%) led to the decrease in both load-carrying and deflection capacities of the strengthened beam, as the CFRP debonding took place earlier than yielding of steel reinforcement.

Hybrid FRP strengthening system for RC bridge superstructures
The hybrid FRP strengthening system comprised of a) prestressed CFRP plates on the soffit of concrete girders and b) prefabricated GFRP panels on the top of the concrete deck. This system was proposed in the research project SUREBRIGE for strengthening the superstructure of existing RC bridges. This hybrid strengthening system was applied to strengthen RC beams (with a T-shaped cross-section) in experimental programme B and evidenced to be a robust and efficient solution for upgrading the flexural performance. In the strengthened RC T-beams subjected to bending, the bottom CFRP plate acted as additional tensile reinforcement and the top GFRP panel took most of the compressive force in the compression zone. The synergy between the CFRP plate and the GFRP panel significantly enhanced the flexural stiffness of the strengthened beams and their load-carrying capacity at debonding of the CFRP plate.

Despite debonding of the CFRP plate, the GFRP panel prevented the concrete crushing at top of the concrete beam and contributed to a substantial residual capacity in the 'post-debonding' phase. Besides the efficiency in structural strengthening, the GFRP panels also provided the opportunity for widening the existing concrete deck.

Bonded-FRP system for deteriorated RC beams
To explore effective FRP-strengthening methods for deteriorated RC beams with corroded steel reinforcement, experimental programme C investigated the bonded-FRP system using externally bonded FRP reinforcement on beam soffits and CFRP U-jackets along the span. The experimental study showed that this bonded-FRP system was efficient in upgrading the load-carrying capacity of deteriorated concrete beams, despite a) maximum local corrosion levels of the steel reinforcement up to 57%, and b) unrepaired concrete cover with corrosion-induced cracks up to 2 mm wide. Further evaluation of the deformation field and cracking within the constant-moment region revealed that the U-jackets effectively suppressed spalling of the concrete cover and thus enabled high utilisation of the bonded FRP on the beam soffits (e.g. the rupture of GFRP laminates in specimens DG1-DG3 or a utilisation ratio of CFRP plates up to 64% in specimens DC1-DC3). The results also highlight the need to evaluate not only the average but also the local corrosion levels of the steel reinforcement. This was conducted in the current work but has not been done in earlier studies on the strengthening of deteriorated RC beams.

In summary, all three FRP-strengthening systems investigated in the current work were evidenced to be robust and efficient in strengthening RC members subjected to bending. This is a result of careful detailing and design of all three systems, which requires good knowledge and understanding of the structural behaviour of both the structure to be strengthened and the applied FRP-strengthening systems.

4.2 Suggestions for future research

The current work provided an insight into the strengthening of existing concrete structures using externally bonded FRP composites. Several areas of importance have been identified for future research:

- The current experimental programmes investigated FRP-strengthening systems in structural tests with monotonic loading. It is of great interest to investigate the performance of strengthened specimens subjected to cyclic loading.

- In the current work, the FRP composites were applied to concrete beams and investigated regarding the short-term performance of strengthened specimens in the laboratory. However, RC structures, e.g. concrete bridges, are commonly exposed to natural weather conditions, such as moisture, freeze-thaw, and solar radiation. Thus, more research is needed to investigate the long-term performance and durability of the bonded FRP composites on concrete structures.
- Although the current work evidenced a high efficiency of using externally bonded FRP composites in upgrading the load-carrying capacity of concrete beams, their deformation capacities were not noticeably improved or even decreased compared to reference specimens. Further studies are needed to investigate possible solutions to improve the deformation capacity and ductility of FRP-strengthened RC structures.
- The current work revealed the importance of the local corrosion level of steel reinforcement to accurately assess the capacity of deteriorated RC members. However, in practice, it is difficult to measure the local corrosion level of reinforcement in existing concrete structures. There is a great demand for developing non-destructive techniques to efficiently detect the local corrosion level of steel reinforcement embedded in concrete members.

References

[1] Pacheco-Torgal F. 1 - Introduction. In: Pacheco-Torgal F, Melchers RE, Shi X, Belie ND, Tittelboom KV, Sáez A, editors. Eco-Efficient Repair and Rehabilitation of Concrete Infrastructures, Woodhead Publishing; 2018, p. 1–12. https://doi.org/10.1016/B978-0-08-102181-1.00001-0.

[2] Kaundinya I, Heimbecher F. Identification and Classification of Relevant European Bridge and Tunnel Types. Taller, Longer, Lighter - Meeting growing demand with limited resources, London: 2011.

[3] Bien J, Elfgren L, Olofsson J. Sustainable bridges: assessment for future traffic demands and longer lives. Wroclaw: Dolnoslaskie Wydawnictwo Edukacyjne; 2007.

[4] PANTURA. D5.3 - Needs for maintenance and refurbishment of bridges in urban environments. 2011.

[5] Mattsson H-Å. Integrated Bridge Maintenance : Evaluation of a pilot project and future perspectives. PhD dissertation. KTH, 2008.

[6] Bakis CE, Bank LC, Brown VL, Cosenza E, Davalos JF, Lesko JJ, et al. Fiber-Reinforced Polymer Composites for Construction—State-of-the-Art Review. J Compos Constr 2002;6:73–87. https://doi.org/10.1061/(ASCE)1090-0268(2002)6:2(73).

[7] Teng JG, Smith ST, Chen JF. 7 - Design guidelines for fibre-reinforced polymer (FRP)-strengthened reinforced concrete (RC) structures. In: Hollaway LC, Teng JG, editors. Strengthening and Rehabilitation of Civil Infrastructures Using Fibre-Reinforced Polymer (FRP) Composites, Woodhead Publishing; 2008, p. 195–214. https://doi.org/10.1533/9781845694890.195.

[8] Hollaway LC. A review of the present and future utilisation of FRP composites in the civil infrastructure with reference to their important in-service properties. Construction and Building Materials 2010;24:2419–45. https://doi.org/10.1016/j.conbuildmat.2010.04.062.

[9] Meier U. Strengthening of structures using carbon fibre/epoxy composites. Construction and Building Materials 1995;9:341–51. https://doi.org/10.1016/0950-0618(95)00071-2.

[10] Meier U. Carbon Fiber-Reinforced Polymers: Modern Materials in Bridge Engineering. Structural Engineering International 1992;2:7–12. https://doi.org/10.2749/101686692780617020.

[11] Täljsten B, Blanksvärd T. Mineral-Based Bonding of Carbon FRP to Strengthen Concrete Structures. Journal of Composites for Construction 2007;11:120–8. https://doi.org/10.1061/(ASCE)1090-0268(2007)11:2(120).

[12] Chen JF, Teng JG. Anchorage strength models for FRP and steel plates bonded to concrete. Journal of Structural Engineering 2001;127:784–91.

[13] Lu XZ, Teng JG, Ye LP, Jiang JJ. Bond–slip models for FRP sheets/plates bonded to concrete. Engineering Structures 2005;27:920–937. https://doi.org/10.1016/j.engstruct.2005.01.014.

[14] Teng JG, Smith ST, Yao J, Chen JF. Intermediate crack-induced debonding in RC beams and slabs. Construction and Building Materials 2003;17:447–62. https://doi.org/10.1016/S0950-0618(03)00043-6.

[15] Dai J, Ueda T, Sato Y. Development of the Nonlinear Bond Stress–Slip Model of Fiber Reinforced Plastics Sheet–Concrete Interfaces with a Simple Method. Journal of Composites for Construction 2005;9:52–62. https://doi.org/10.1061/(ASCE)1090-0268(2005)9:1(52).

[16] Sas G, Täljsten B, Barros J, Lima J, Carolin A. Are Available Models Reliable for Predicting the FRP Contribution to the Shear Resistance of RC Beams? Journal of

Composites for Construction 2009;13:514–34. https://doi.org/10.1061/(ASCE)CC.1943-5614.0000045.
[17] Kotynia R, Abdel Baky H, Neale KW, Ebead UA. Flexural Strengthening of RC Beams with Externally Bonded CFRP Systems: Test Results and 3D Nonlinear FE Analysis. Journal of Composites for Construction 2008;12:190–201. https://doi.org/10.1061/(ASCE)1090-0268(2008)12:2(190).
[18] Triantafillou TC. Shear Strengthening of Reinforced Concrete Beams Using Epoxy-Bonded FRP Composites. SJ 1998;95:107–15. https://doi.org/10.14359/531.
[19] El-Hacha R, Wight RG, Green MF. Innovative System for Prestressing Fiber-Reinforced Polymer Sheets. SJ 2003;100:305–13.
[20] Täljsten B. Defining anchor lengths of steel and CFRP plates bonded to concrete. International Journal of Adhesion and Adhesives 1997;17:319–27. https://doi.org/10.1016/S0143-7496(97)00018-3.
[21] Triantafillou TC, Deskovic N. Innovative Prestressing with FRP Sheets: Mechanics of Short-Term Behavior. J Eng Mech 1991;117:1652–72. https://doi.org/10.1061/(ASCE)0733-9399(1991)117:7(1652).
[22] Triantafillou TC, Deskovic N, Deuring M. Strengthening of concrete structures with prestressed fiber reinforced plastic sheets. ACI Structural Journal 1992;89:235–44.
[23] El-Hacha R, Aly MYE. Anchorage System to Prestress FRP Laminates for Flexural Strengthening of Steel-Concrete Composite Girders. Journal of Composites for Construction 2013;17:324–35. https://doi.org/10.1061/(ASCE)CC.1943-5614.0000323.
[24] Grelle SV, Sneed LH. Review of Anchorage Systems for Externally Bonded FRP Laminates. International Journal of Concrete Structures and Materials 2013;7:17–33. https://doi.org/10.1007/s40069-013-0029-0.
[25] SUREBRIDGE–Sustainable Refurbishment of Existing Bridges n.d. http://surebridge.eu/ (accessed February 19, 2021).
[26] Haddad RH. Hybrid repair configurations with CFRP composites for recovering structural performance of steel-corroded beams. Construction and Building Materials 2016;124:508–18. https://doi.org/10.1016/j.conbuildmat.2016.07.124.
[27] Al-Saidy AH, Al-Jabri KS. Effect of damaged concrete cover on the behavior of corroded concrete beams repaired with CFRP sheets. Composite Structures 2011;93:1775–86. https://doi.org/10.1016/j.compstruct.2011.01.011.
[28] Al-Saidy AH, Saadatmanesh H, El-Gamal S, Al-Jabri KS, Waris BM. Structural behavior of corroded RC beams with/without stirrups repaired with CFRP sheets. Materials and Structures/Materiaux et Constructions 2016;49:3733–47. https://doi.org/10.1617/s11527-015-0751-y.
[29] Katsumata H, Kobatake Y, Takeda T. A study on the strengthening with carbon fiber for earthquake-resistant capacity of existing reinforced concrete columns. Proceedings of 9th World Conference on Earthquake Engineering, vol. 7, Tokyo-Kyoto, Japen: 1988, p. 518–22.
[30] Bournas DA, Lontou PV, Papanicolaou CG, Triantafillou TC. Textile-Reinforced Mortar versus Fiber-Reinforced Polymer Confinement in Reinforced Concrete Columns. SJ 2007;104:740–8. https://doi.org/10.14359/18956.
[31] fib TG 9.3. fib Bulletin 14 : Externally applied FRP reinforcement for concrete structures. International Federation for Structural Concrete; 2001.
[32] fib T5.1. fib Bulletin 90: Externally applied FRP reinforcement for concrete structures. International Federation for Structural Concrete; 2019.
[33] CNR. CNR-DT 200 R1/2013: Guide for the Design and Construction of Externally Bonded FRP Systems for Strengthening Existing Structures. Roma, Italy: CNR; 2014.

[34] Concrete Society. TR55-Design guidance for strengthening concrete structures using fibre composite materials (3rd edition). Camberley, UK: Concrete Society; 2012.
[35] ACI Committee 440. ACI PRC-440.2-17: Guide for the Design and Construction of Externally Bonded FRP Systems for Strengthening Concrete Structures. USA: American Concrete Institute; 2017.
[36] CSA. CSA S806 - Design and construction of building structures with fibre-reinforced polymers | Engineering360. Canadian Standards Association; 2012.
[37] Concrete Engineering Series 41. JSCE: Recommendations for upgrading of concrete structures with use of continuous fiber sheets. Tokyo, Japan: Japan Society of Civil Engineers; 2001.
[38] Teng JG, Chen JF, Smith ST, Lam L. FRP-Strengthened RC Structures. Chichester, UK: John Wiley & Sons; 2002.
[39] Täljsten B, Blanksvärd T, Gabriel S. kompositförstärkning av betong. Svensk Byggtjänst; 2016.
[40] Motavalli M, Czaderski C, Pfyl-Lang K. Prestressed CFRP for Strengthening of Reinforced Concrete Structures: Recent Developments at Empa, Switzerland. Journal of Composites for Construction 2011;15:194–205. https://doi.org/10.1061/(ASCE)CC.1943-5614.0000125.
[41] Kotynia R, Lasek K, Staskiewicz M. Flexural Behavior of Preloaded RC Slabs Strengthened with Prestressed CFRP Laminates. Journal of Composites for Construction 2014;18:A4013004. https://doi.org/10.1061/(ASCE)CC.1943-5614.0000421.
[42] El Maaddawy Tamer, Soudki Khaled. Carbon-Fiber-Reinforced Polymer Repair to Extend Service Life of Corroded Reinforced Concrete Beams. Journal of Composites for Construction 2005;9:187–94. https://doi.org/10.1061/(ASCE)1090-0268(2005)9:2(187).
[43] Benjeddou O, Ouezdou MB, Bedday A. Damaged RC beams repaired by bonding of CFRP laminates. Construction and Building Materials 2007;21:1301–10. https://doi.org/10.1016/j.conbuildmat.2006.01.008.
[44] Bergström M. Assessment of existing concrete bridges: bending stiffness as a performance indicator. 2009.
[45] Fayyadh MM, Abdul Razak H. Assessment of effectiveness of CFRP repaired RC beams under different damage levels based on flexural stiffness. Construction and Building Materials 2012;37:125–34. https://doi.org/10.1016/j.conbuildmat.2012.07.021.
[46] Xie J, Hu R. Experimental study on rehabilitation of corrosion-damaged reinforced concrete beams with carbon fiber reinforced polymer. Construction and Building Materials 2013;38:708–16. https://doi.org/10.1016/j.conbuildmat.2012.09.023.
[47] Almassri B, Kreit A, Mahmoud FA, François R. Mechanical behaviour of corroded RC beams strengthened by NSM CFRP rods. Composites Part B: Engineering 2014;64:97–107. https://doi.org/10.1016/j.compositesb.2014.04.012.
[48] Elghazy M, El Refai A, Ebead U, Nanni A. Effect of corrosion damage on the flexural performance of RC beams strengthened with FRCM composites. Composite Structures 2017;180:994–1006. https://doi.org/10.1016/j.compstruct.2017.08.069.
[49] Siad A, Bencheikh M, Hussein L. Effect of combined pre-cracking and corrosion on the method of repair of concrete beams. Construction and Building Materials 2017;132:462–9. https://doi.org/10.1016/j.conbuildmat.2016.12.020.
[50] Triantafyllou GG, Rousakis TC, Karabinis AI. Effect of patch repair and strengthening with EBR and NSM CFRP laminates for RC beams with low, medium and heavy corrosion. Composites Part B: Engineering 2018;133:101–11. https://doi.org/10.1016/j.compositesb.2017.09.029.

[51] Liu X, Li Y. Static bearing capacity of partially corrosion-damaged reinforced concrete structures strengthened with PET FRP composites. Construction and Building Materials 2019;211:33–43. https://doi.org/10.1016/j.conbuildmat.2019.03.218.
[52] Haghani R, Al-Emrani M, Kliger R. A new method for strengthening concrete structures using prestressed FRP laminates. Proceeding of the 8th International Structural Engineering and Construction Conference, 2015, p. 1153–8.
[53] Haghani R, Al-Emrani M. A new method for application of pre-stressed FRP laminates for strengthening of concrete structures. Proceeding of the 19th IABSE Congress, Stockholm: 2016, p. 1556–63.
[54] Al-Emrani M, Kliger R. Analysis of interfacial shear stresses in beams strengthened with bonded prestressed laminates. Composites Part B: Engineering 2006;37:265–72. https://doi.org/10.1016/j.compositesb.2006.01.004.
[55] Haghani R, Al-Emrani M, Kliger R. Interfacial stress analysis of geometrically modified adhesive joints in steel beams strengthened with FRP laminates. Construction and Building Materials 2009;23:1413–22. https://doi.org/10.1016/j.conbuildmat.2008.07.013.
[56] Yang J, Haghani R, Al-Emrani M. Innovative prestressing method for externally bonded CFRP laminates without mechanical anchorage. Engineering Structures 2019;197:109416. https://doi.org/10.1016/j.engstruct.2019.109416.
[57] Fu B, Tang XT, Li LJ, Liu F, Lin G. Inclined FRP U-jackets for enhancing structural performance of FRP-plated RC beams suffering from IC debonding. Composite Structures 2018;200:36–46. https://doi.org/10.1016/j.compstruct.2018.05.074.
[58] Simulia. ABAQUS/Standard 6.14. Providence, RI: Dassault Systems; 2014.
[59] fib. CEB-FIP Model Code 1990: Design Code. fib Fédération internationale du béton; 1993.
[60] fib. fib Model Code for Concrete Structures 2010. John Wiley & Sons; 2013.
[61] Fernandez I, Lundgren K, Zandi K. Evaluation of corrosion level of naturally corroded bars using different cleaning methods, computed tomography, and 3D optical scanning. Mater Struct 2018;51:78. https://doi.org/10.1617/s11527-018-1206-z.
[62] Fernandez I, Berrocal CG. Mechanical Properties of 30 Year-Old Naturally Corroded Steel Reinforcing Bars. Int J Concr Struct Mater 2019;13:9. https://doi.org/10.1186/s40069-018-0308-x.
[63] Chen E, Berrocal CG, Fernandez I, Löfgren I, Lundgren K. Assessment of the mechanical behaviour of reinforcement bars with localised pitting corrosion by Digital Image Correlation. Engineering Structures 2020;219:110936. https://doi.org/10.1016/j.engstruct.2020.110936.

APPENDICES

Appendix A: Supplementary experimental data

The appendix encompasses experimental data of **experimental programmes C**, which has not been presented in the main body of this thesis nor in the appended papers.

1 Concrete and steel reinforcement

Ready-mix concrete was order and used to cast the ten beams in the laboratory at Chalmers University of Technology. The material properties of concrete according to standard tests are summarised in Table A.1. The position of the tensile and compressive steel reinforcement in the RC beams were measured before the casting, see Table A.2. The mechanical properties of steel bars used as tensile reinforcement, compressive reinforcement, and stirrups are presented, respectively, in Table A.3, A.4, and A.5

Table A.1. Material properties of concrete

Date of casting	2019-11-19	2019-11-19	2019-11-19	2019-11-19
Date of testing	2019-12-17	2020-09-07	2020-09-07	2020-09-04
Samples	$f_{cm.28}$ [MPa]	$f_{cm.t}$ [MPa]	$E_{cm.t}$ [GPa]	G_F [N/m]
1	65.0	80.6	32.7	124.2
2	67.1	74.1	36.1	149.2
3	72.5	81.4	31.0	129.5
Mean value	68.2	78.7	33.3	134.3
SD	3.9	4.0	2.6	10.7
COV	5.7%	5.0%	7.7	8.0%

Notations:

$f_{cm.28}$–*the compressive strength of concrete cubes (150×150×150 mm3) on 28 days according to SS-EN 12390-3:2019;*

$f_{cm.t}$–*the compressive strength of concrete cubes (150×150×150 mm3) in the week of final structural tests according to SS-EN 12390-3:2019;*

$E_{cm.t}$–*the modulus of elasticity of concrete cylinders (diameter 50 mm, height 200 mm) in the week of final structural tests according to SS-EN 12390-13:2013;*

G_F–*the fracture energy of concrete in the week of final structural tests based on wedge-splitting tests using the configuration described in Lövgren et al. (2004);*

SD–*standard deviation;*

COV–*coefficient of variation: the ratio of the standard deviation to the mean value.*

Table A.2. Position of tensile and compressive steel reinforcement in the beam specimens

Specimens	h_{st} [mm]	h_{sc} [mm]
RN1	41	190
RN2	40	189
DN1	40	191
DN2	N.A.	N.A.
DG1	39	189
DG2	39	190
DG3	38	190
DC1	38	189
DC2	39	191
DC3	41	192
Mean value	39.4	190.2

Notations:

h_{st} –*distance between the bottom surface of beam and the centre of tensile steel reinforcement;*

h_{sc} –distance between the bottom surface of beam and the centre of compressive steel reinforcement;
N.A.–data not available.

Table A.3. Standard tensile tests of steel bars (Φ12) used as tensile reinforcement

Samples Φ12	E_s [GPa]	σ_{sy} [MPa]	σ_{su} [MPa]	ε_{su} [%]
1	190.9	583.9	671.9	8.41
2	195.4	569.2	663.4	8.94
3	186.6	568.4	660.7	7.40
4	196.1	570.5	660.3	7.83
5	191.8	562.1	655.9	8.65
6	188.1	564.5	653.6	7.31
Mean value	191	570	661	8.1
SD	3.5	6.9	5.9	0.6
COV	1.8%	1.2%	0.9%	7.6%

Notations: E_s – the modulus of elasticity; σ_{sy} –yield strength; σ_{su} and ε_{su} –ultimate tensile strength and strain when reaching the maximum tensile force; SD*–standard deviation;* COV*–coefficient of variation: the ratio of the standard deviation to the mean value.*

Table A.4. Standard tensile tests of steel bars (Φ10) used as compressive reinforcement

Samples Φ10	E_s [GPa]	σ_{sy} [MPa]	σ_{su} [MPa]	ε_{su} [%]
1	207.8	530.8	630.3	9.06
2	195.2	523.9	627.8	10.43
3	198.5	528.3	632.7	10.06
4	197.2	526.6	628.3	7.41
5	201.9	531.6	633.0	7.60
Mean value	200	528	630	8.9
SD	4.4	2.8	2.2	1.2
COV	2.2%	0.5%	0.3%	13.8%

Notations: same as Table A.3.

Table A.5. Standard tensile tests of steel bars (Φ8) used as stirrups

Samples Φ8	E_s [GPa]	σ_{sy} [MPa]	σ_{su} [MPa]	ε_{su} [%]
1	205.4	529.5	652.2	10.66
2	200.6	531.9	659.8	10.17
3	209.8	533.2	647.2	7.91
4	193.0	530.8	655.3	9.57
Mean value	202	531	654	9.6
SD	6.2	1.4	4.6	1.0
COV	3.1%	0.3%	0.7%	10.8%

Notations: same as Table A.3.

2 GFRP laminates and CFRP U-jackets

The bonded-FRP strengthening system applied to the six specimens in groups DG and DC include the use of CFRP plates and GFRP laminates as externally bonded flexural reinforcement and CFRP U-jackets along the span for transverse confinement. The GFRP laminates and CFRP U-jackets were bonded with wet lay-up methods. Based on the standard tensile tests of dog-bone samples, the mechanical properties of the GFRP laminates and CFRP U-jackets are shown in Table A.6.

Table A.6. Mechanical properties of the GFRP laminates and CFRP U-jackets made by wet lay-up methods

Samples	E_{gf} [GPa]	ε_{gfu} [%]	E_{cf} [GPa]	ε_{cfu} [%]
1	20.27	1.84	53.64	1.22
2	20.02	1.82	57.52	1.33
3	20.22	1.76	55.87	1.32
4	20.31	1.85	59.87	1.25
5	20.34	1.72	60.89	1.10
6	20.16	1.91	57.97	1.20
Mean value	20.22	1.82	57.63	1.24
COV	0.5%	3.4%	4.2%	6.2%

Notations:

E_{gf} *and* ε_{gfu} *–the elastic modulus and ultimate tensile strain of GFRP laminates externally bonded on the soffit of specimens in group DG;*

E_{cf} *and* ε_{cfu} *–the elastic modulus and ultimate tensile strain of CFRP U-jackets bonded along the span of specimens in groups DG and DC;*

COV*–coefficient of variation: the ratio of the standard deviation to the mean value.*

3 Flexural cracks induced by pre-loading

After three weeks of curing, the eight beams in groups DN, DG, and DC were subjected to three-point bending with an effective span of 1.8 meters and pre-loaded to 25.2 kN, equivalent to 60% of the theoretical yielding load. Five to six cracks were induced in the mid-region of the beams. Figure A.1a shows the crack widths measured on the front face of the beam close to the bottom edge under the maximum pre-load. After removing the pre-load, crack widths in the mid-400-mm region decreased significantly. Figure A.1b shows the crack widths on the bottom surfaces of the eight beams measured one day after the pre-loading.

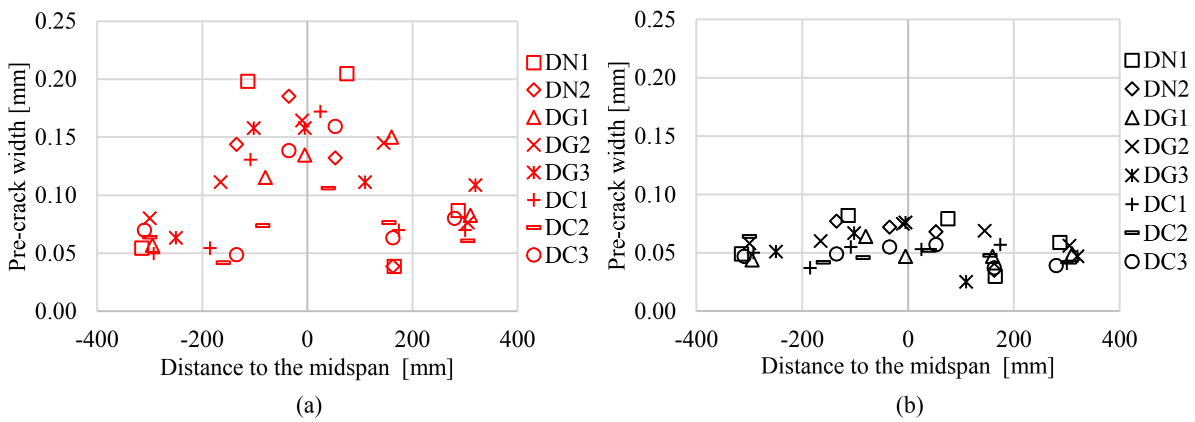

Figure A.1. The widths of flexural cracks induced by the pre-loading measured (a) on the front face of the beam close to the bottom edge and (b) on the bottom surface of the beam one day after the pre-loading

4 Corrosion of steel reinforcement and corrosion-induced cracks

Figures A.2-A.9 show the cross-sectional area of tensile reinforcement in the initial and corroded states, the pattern of corrosion-induced cracks, and the width of corrosion-induced cracks measured every 150 mm for each of the deteriorated specimens in groups DN, DG, and DC.

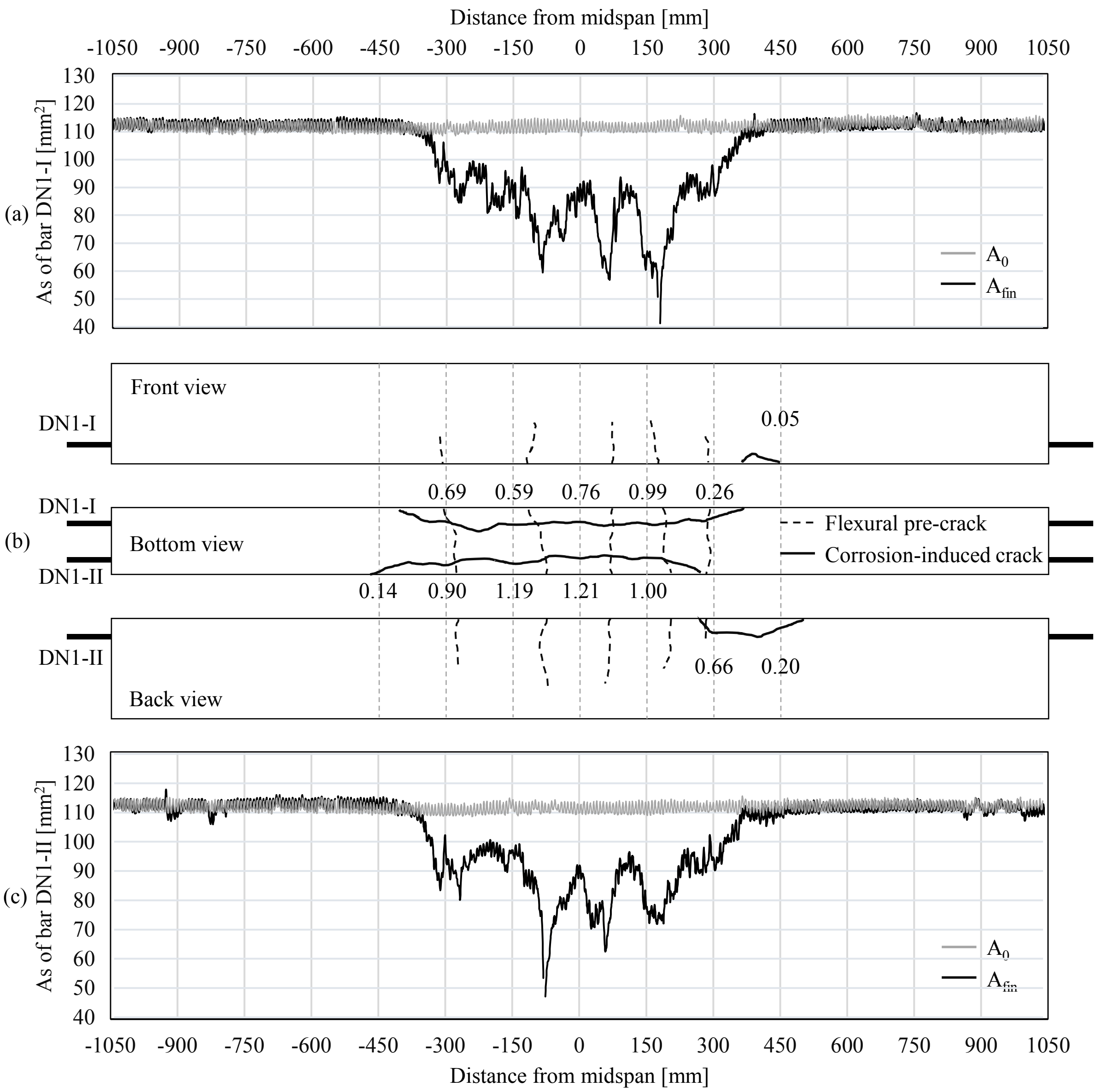

Figure A.2. (a, c) Cross-sectional areas of the tensile reinforcement bars I and II in specimen DN1; (b) flexural pre-cracks and corrosion induced cracks, of which the widths (unit in mm) were measured every 150 mm; As–cross-sectional area; A_0–cross-sectional area of steel bars measured in the initial state before casting beams; A_{fin}–cross-sectional area of steel bars measured in the final state after taken out from the tested specimens.

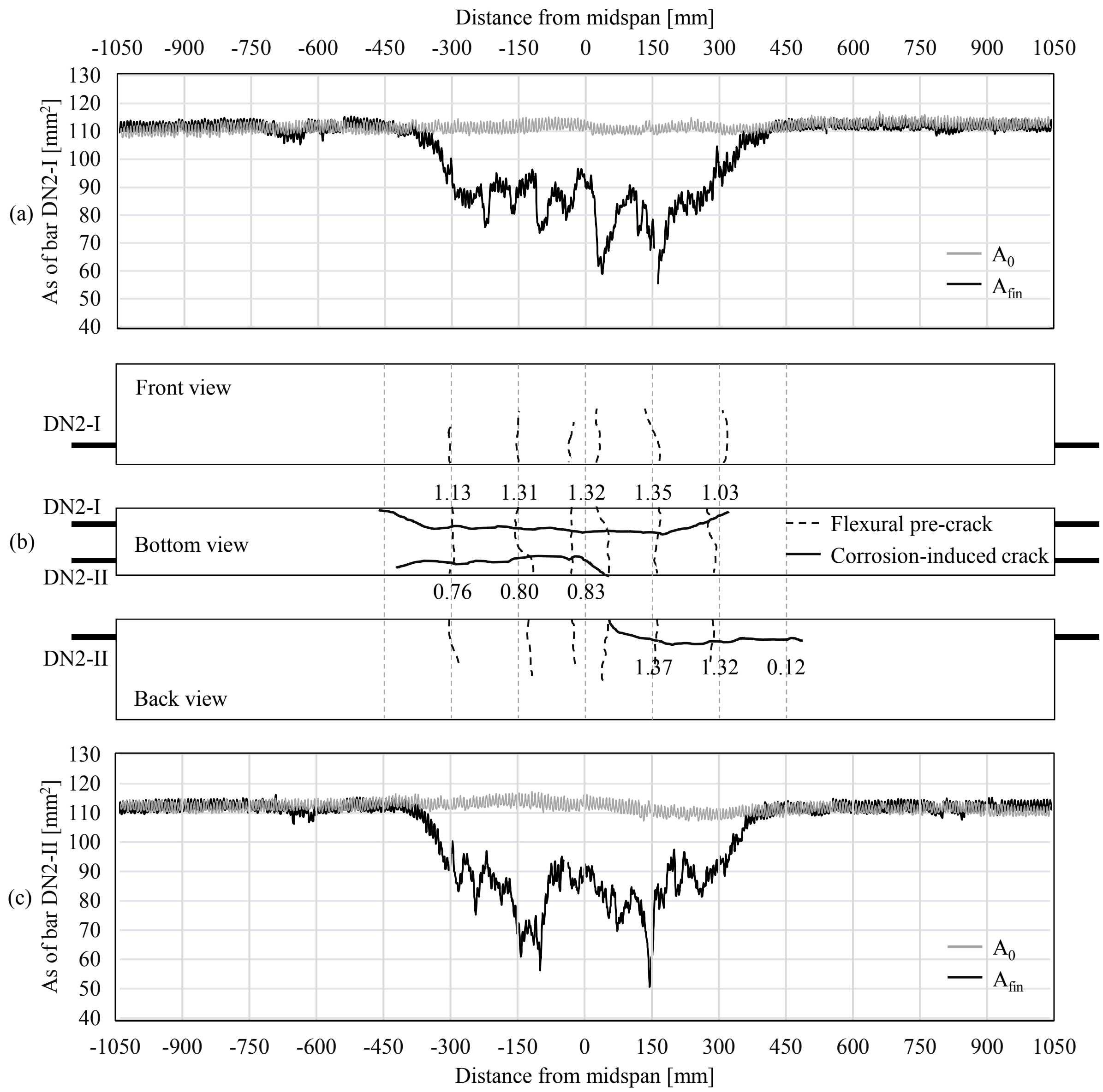

Figure A.3. (a, c) Cross-sectional areas of the tensile reinforcement bars I and II in specimen DN2; (b) flexural pre-cracks and corrosion induced cracks, of which the widths (unit in mm) were measured every 150 mm; As–cross-sectional area; A_0–cross-sectional area of steel bars measured in the initial state before casting beams; A_{fin}–cross-sectional area of steel bars measured in the final state after taken out from the tested specimens.

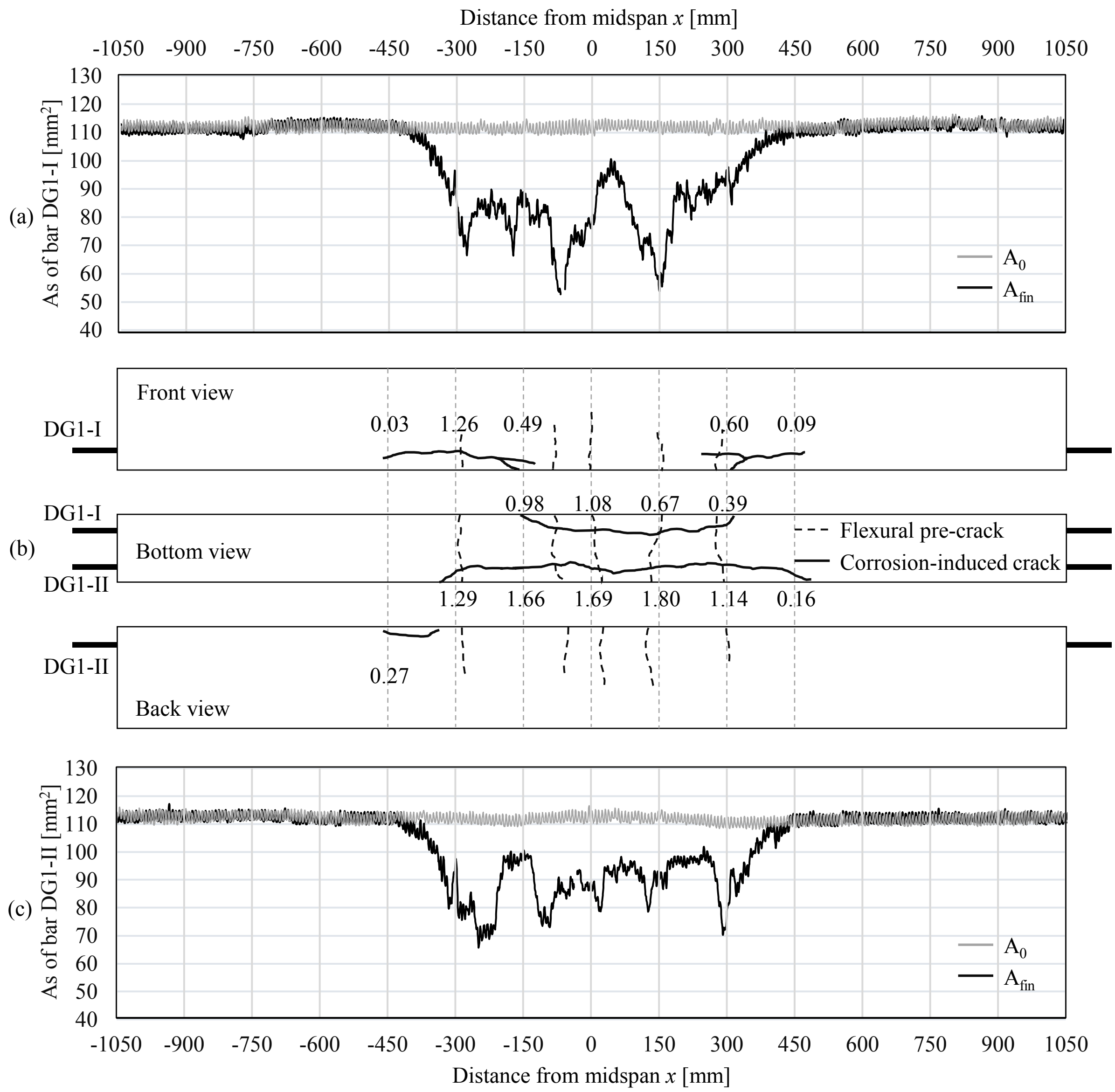

Figure A.4. (a, c) Cross-sectional areas of the tensile reinforcement bars I and II in specimen DG1; (b) flexural pre-cracks and corrosion induced cracks, of which the widths (unit in mm) were measured every 150 mm; As–cross-sectional area; A_0–cross-sectional area of steel bars measured in the initial state before casting beams; A_{fin}–cross-sectional area of steel bars measured in the final state after taken out from the tested specimens.

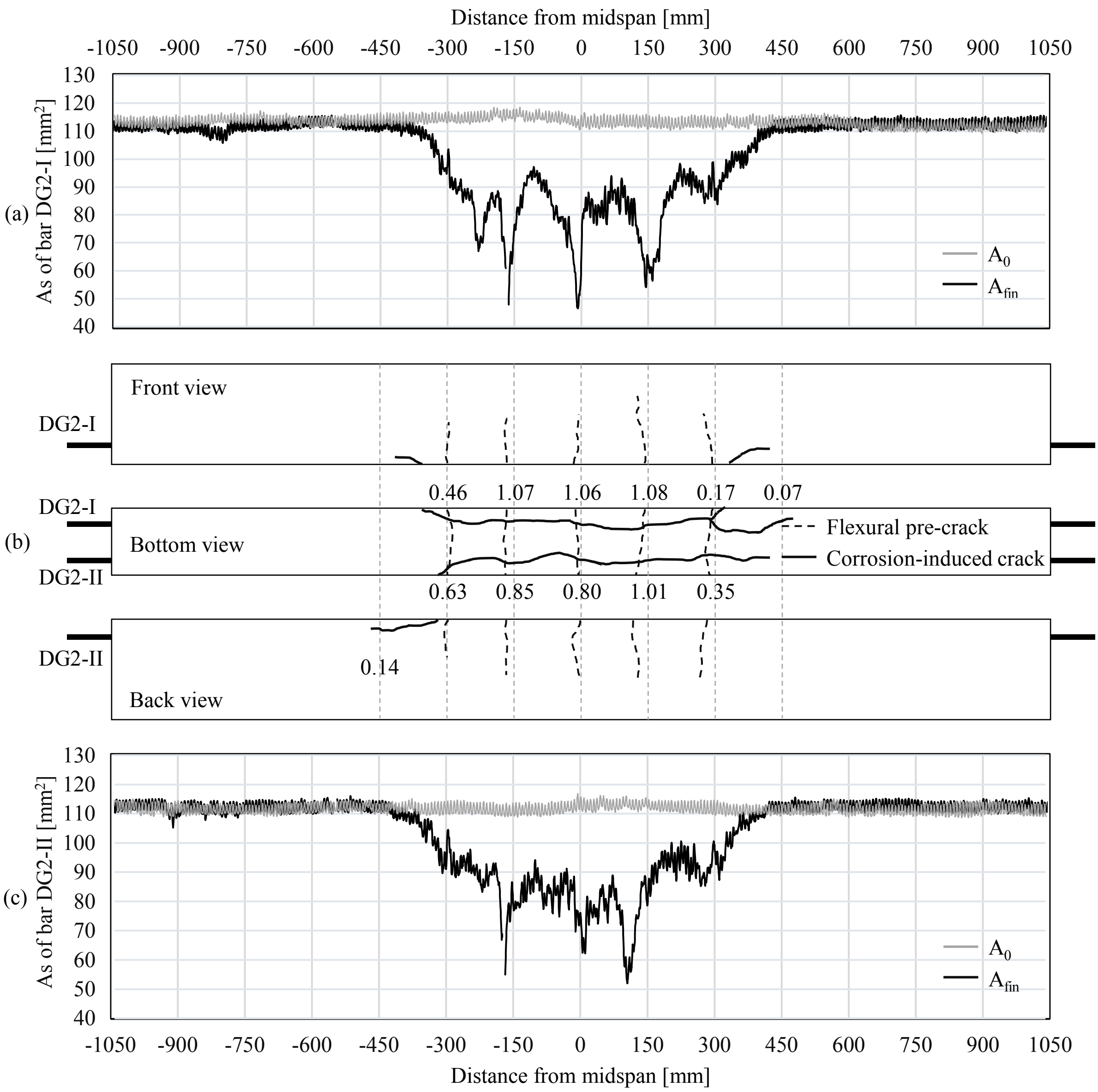

Figure A.5. (a, c) Cross-sectional areas of the tensile reinforcement bars I and II in specimen DG2; (b) flexural pre-cracks and corrosion induced cracks, of which the widths (unit in mm) were measured every 150 mm; As–cross-sectional area; A_0–cross-sectional area of steel bars measured in the initial state before casting beams; A_{fin}–cross-sectional area of steel bars measured in the final state after taken out from the tested specimens.

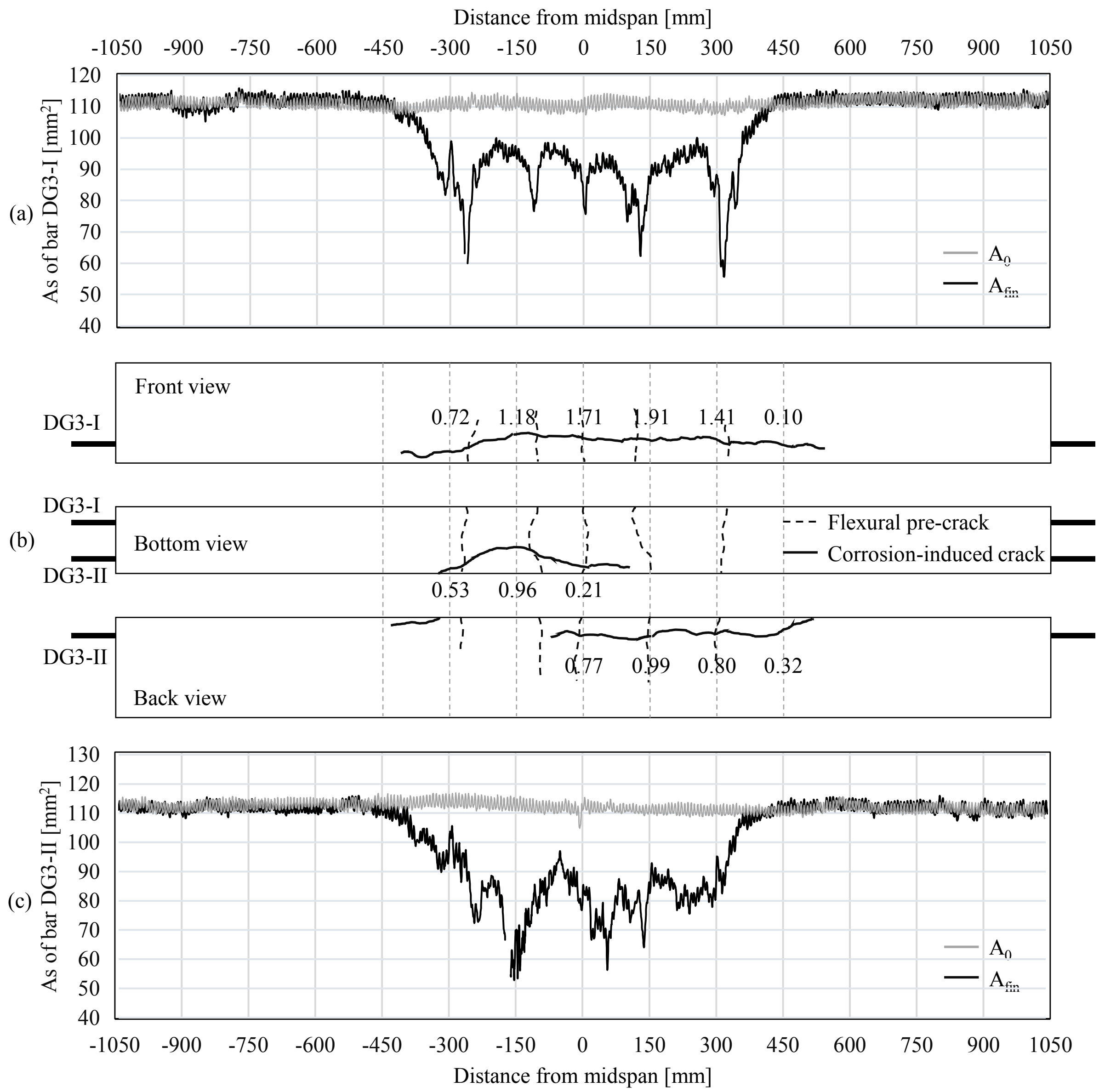

Figure A.6. (a, c) Cross-sectional areas of the tensile reinforcement bars I and II in specimen DG3; (b) flexural pre-cracks and corrosion induced cracks, of which the widths (unit in mm) were measured every 150 mm; As–cross-sectional area; A_0–cross-sectional area of steel bars measured in the initial state before casting beams; A_{fin}–cross-sectional area of steel bars measured in the final state after taken out from the tested specimens.

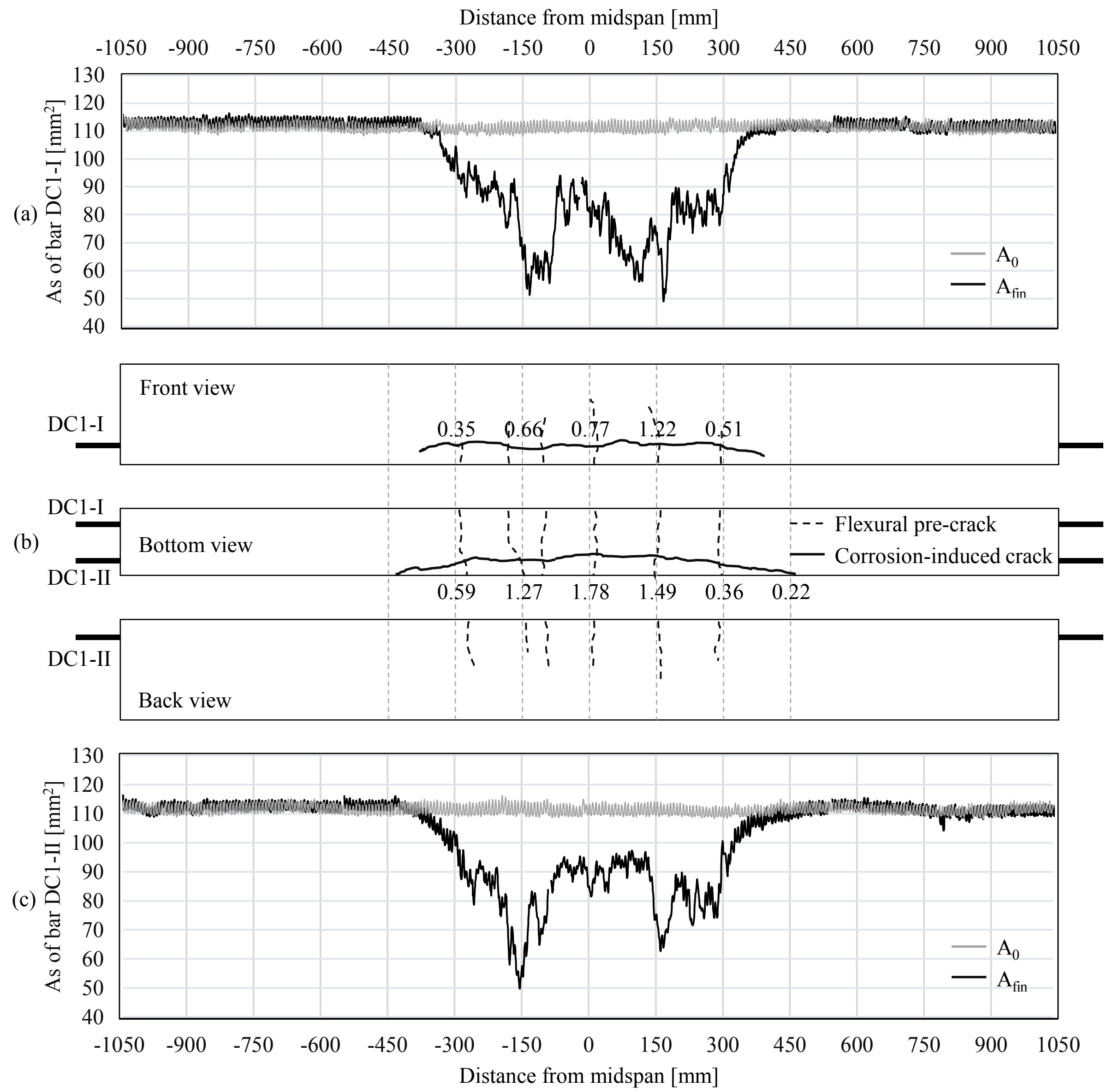

Figure A.7. (a, c) Cross-sectional areas of the tensile reinforcement bars I and II in specimen DC1; (b) flexural pre-cracks and corrosion induced cracks, of which the widths (unit in mm) were measured every 150 mm; As–cross-sectional area; A_0–cross-sectional area of steel bars measured in the initial state before casting beams; A_{fin}–cross-sectional area of steel bars measured in the final state after taken out from the tested specimens.

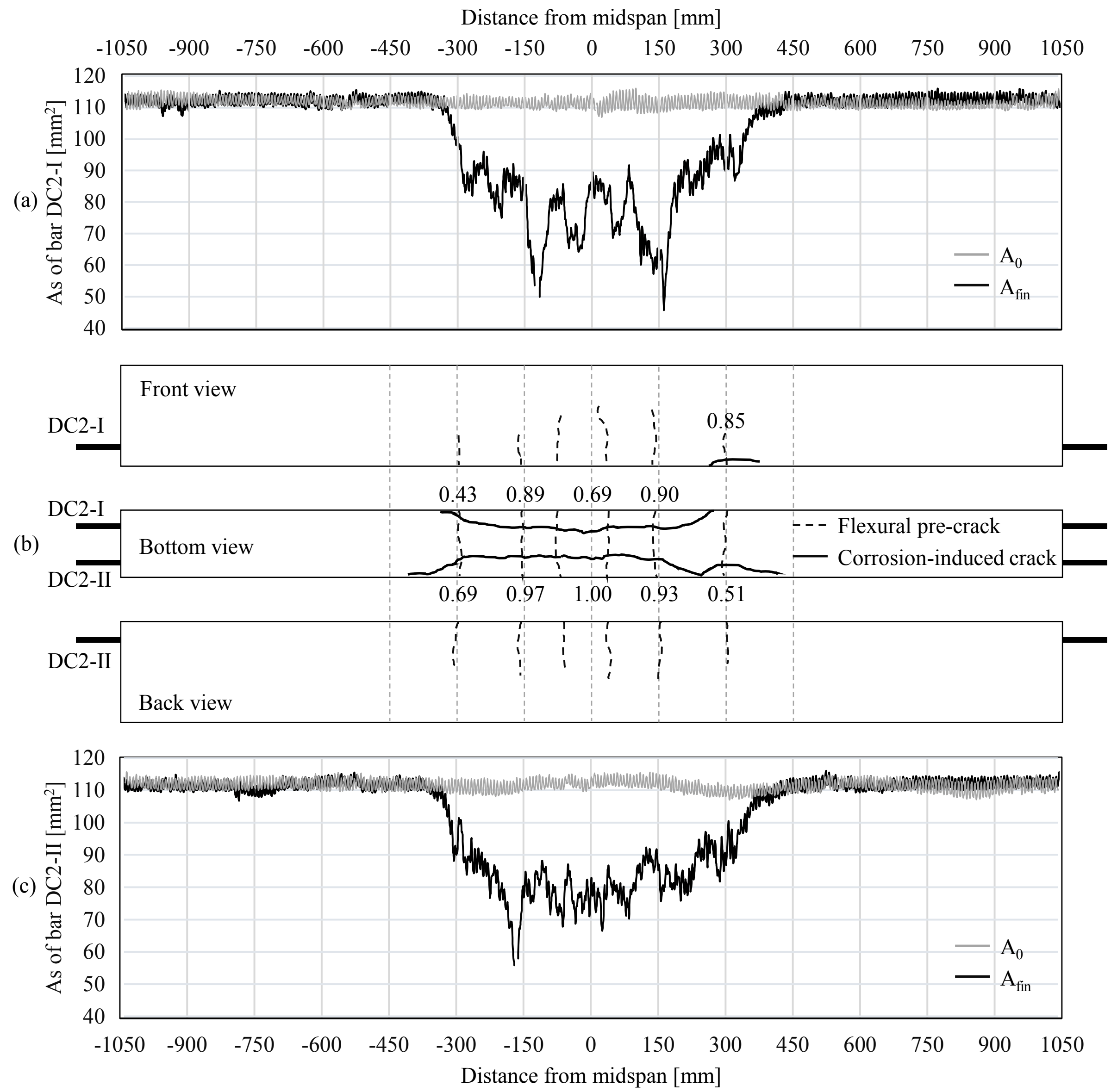

Figure A.8. (a, c) Cross-sectional areas of the tensile reinforcement bars I and II in specimen DC2; (b) flexural pre-cracks and corrosion induced cracks, of which the widths (unit in mm) were measured every 150 mm; As–cross-sectional area; A_0–cross-sectional area of steel bars measured in the initial state before casting beams; A_{fin}–cross-sectional area of steel bars measured in the final state after taken out from the tested specimens.

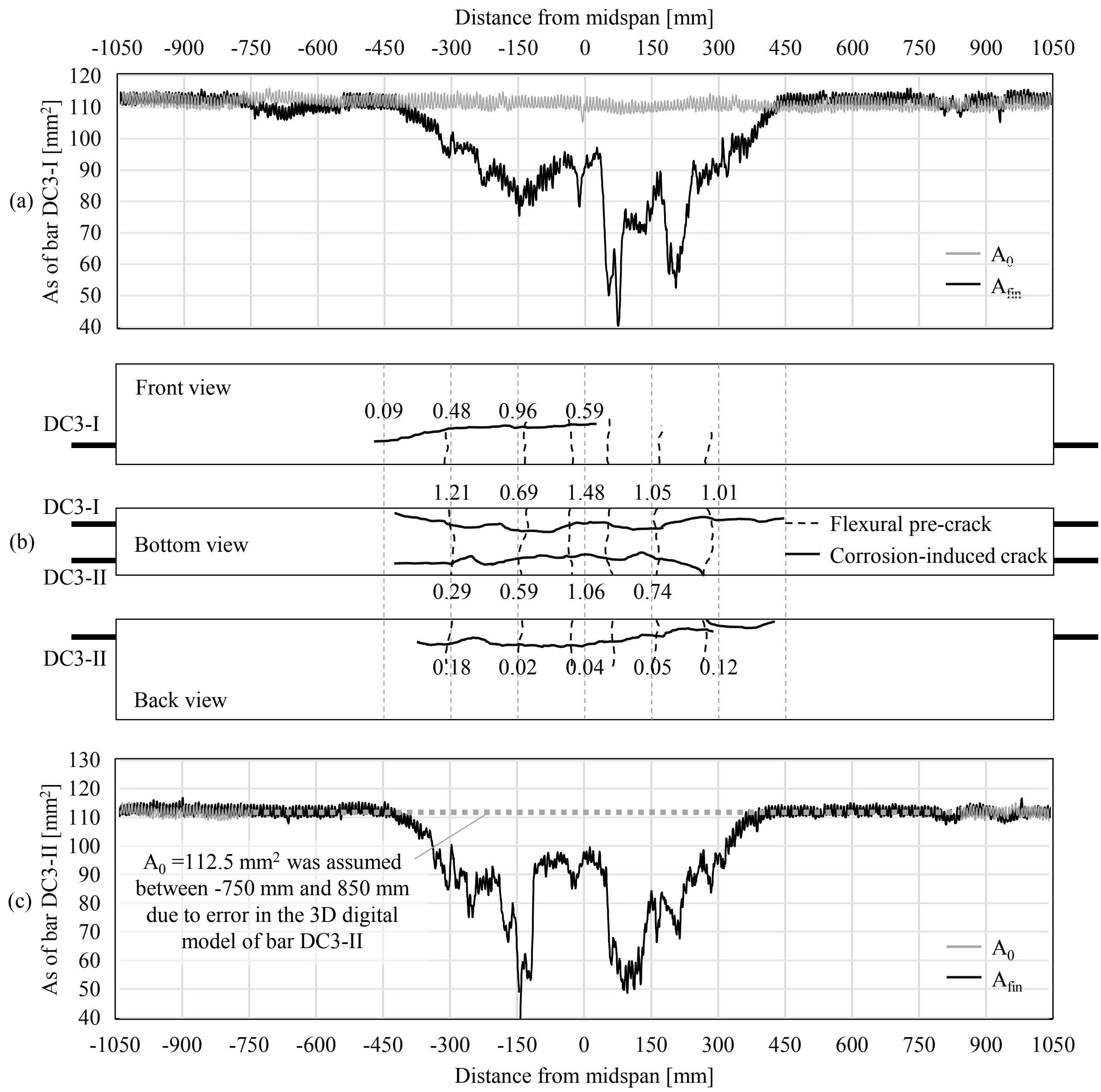

Figure A.9. (a, c) Cross-sectional areas of the tensile reinforcement bars I and II in specimen DC3; (b) flexural pre-cracks and corrosion induced cracks, of which the widths (unit in mm) were measured every 150 mm; As–cross-sectional area; A_0–cross-sectional area of steel bars measured in the initial state before casting beams; A_{fin}–cross-sectional area of steel bars measured in the final state after taken out from the tested specimens.